ECLIPSE

EFFICIENT CRYOGENIC LOW INVASIVE PROPELLANT SUPPLY EXCHANGE

2025 HuLC

The Grainger College of Engineering
UNIVERSITY OF ILLINOIS URBANA-CHAMPAIGN

Faculty Advisor: Dr. Vishwanath Ganesan
Project Manager: Cliff Sun

Aneesh Ganti | Braedyn Kim | Charles Cundiff | Divij Garg
Robert Barthell | Thach Dang | John Galleta | Jett Haas
Keaton Jones | Justin Kotrba | Anna Lambros
Michael Milowski | Sebastian Moreno | Zahi Rahman
Sebastian Rojas | Anna Rudenko | Nate Vattana

Agenda

Overview

- Cryogenics Background
- Objective
- Value Proposition
- Mission Timeline

Concept of Operations

- Line Chilldown
- Tank Chilldown
- Propellant Transfer

Mission Assessment

- Cost Analysis
- Test Campaign
- Risk Analysis
- Key Innovations

Intro to Cryogenic Propellant Transfer

- **Importance?** Cryogenic liquids in the HLS mission architecture must be efficiently and safely transferred in microgravity
- **Issues?** Propellant boil-off during transfer reduces useable propellant and risks tank over-pressurization
- **Impact?** Proper boil-off mitigations techniques reduce propellant loss and improve transfer safety in support of long-duration missions

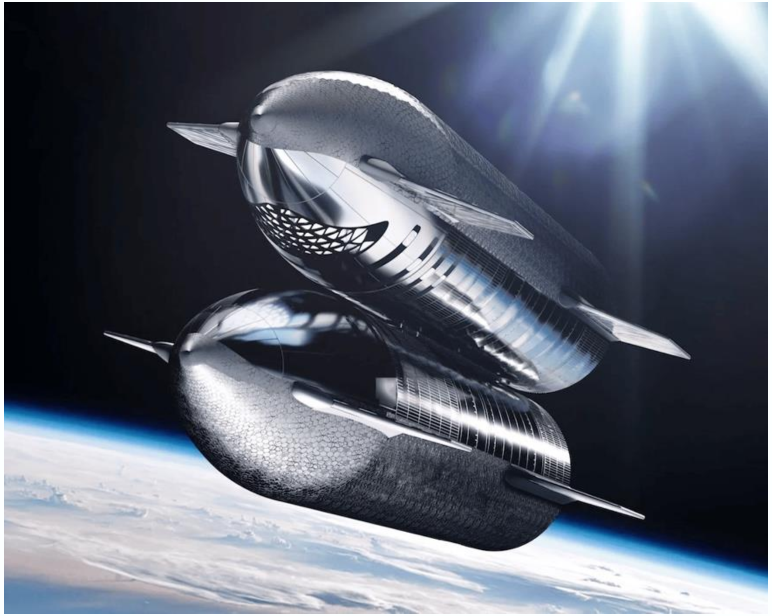

Cryogenic Background and Impacts

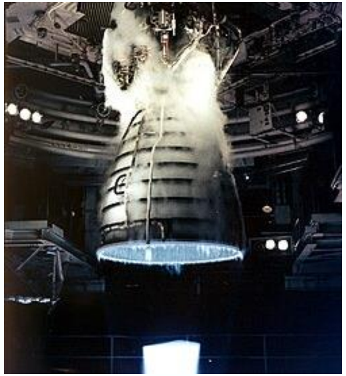

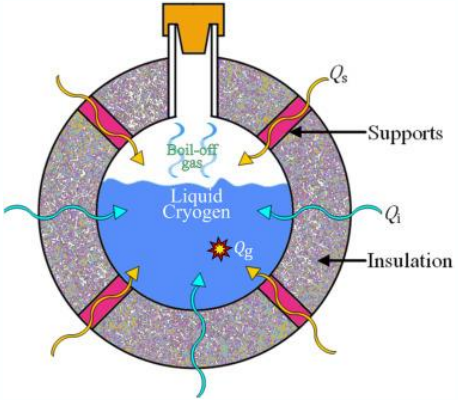

Propellant Losses

- Directly impact long-duration missions
- Jeopardize transfer timeline

Tank Over-Pressurization

- Critically endangers HLS architecture and crew
- Damages surrounding tank structure and instrumentation

Transfer Line Heat Leaks

- Compromise efficiency of one-phase propellant transfer
- Result in unintended gas entering storage tank

Goal

Address gaps in existing research:

- Holistic cryogenic transfer protocol
- Propellant line flow monitoring
- HLS architecture health

Strategy

Direct research efforts towards:

- Line Childown
- Tank Childown
- 2-Phase Flow Imaging

Goal: Monitor and manage boil-off during transfer

The University of Illinois proposes ECLIPSE, which will:

- **Mitigate propellant losses** during line chilldown through transfer line coatings and pulsed propellant flow
- **Reduce tank over-pressurization risks** through operational changes in the tank chilldown protocol
- **Monitor heat leaks** along the transfer line with a flow-monitoring sensor

Concept of Operations

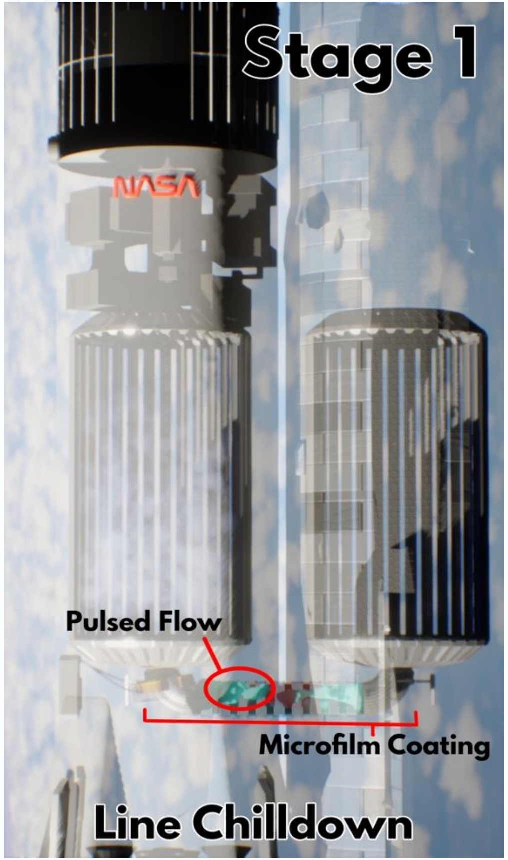

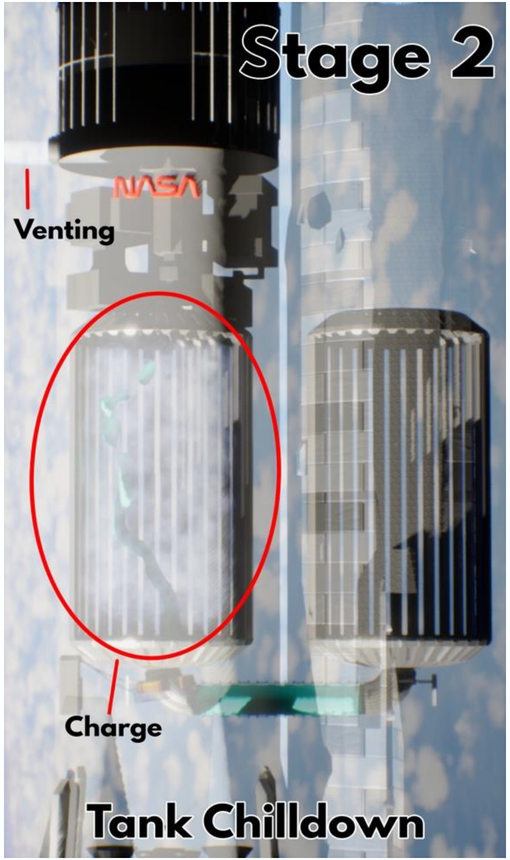

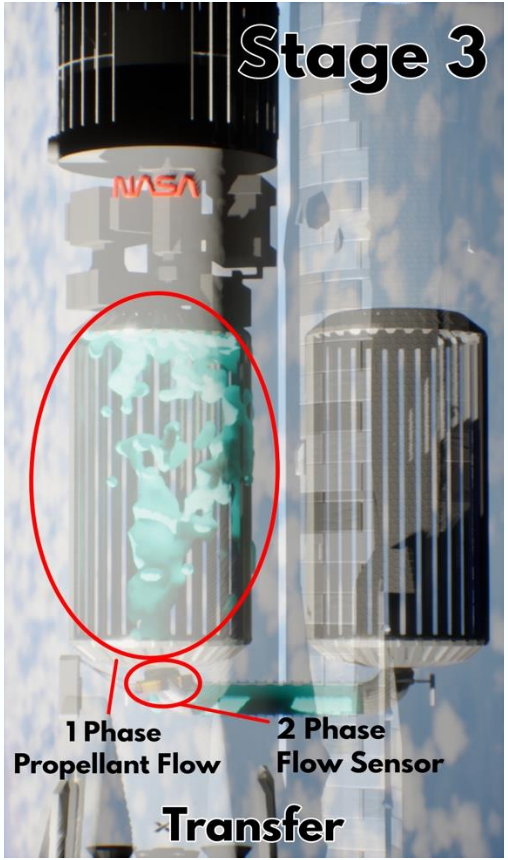

Mission Timeline

Key Goals

- Develop mission concept and integration
- Verify concept with simulations

Mission Milestones

- MCR
- SRR
- MDR
- PDR

Key Goals

- Develop and test each component of ECLIPSE
- Refine fabrication processes

Mission Milestones

- CDR
- ORR

Key Goals

- Run precursor mission
- Refine simulations based on precursor
- Launch first mission

Mission Milestones

- PLAR
- FRR

2025
Concept Studies

2026 – 2027
Project Development

2028 - 2029
Mission Operations

Stage 1: Line Chilldown

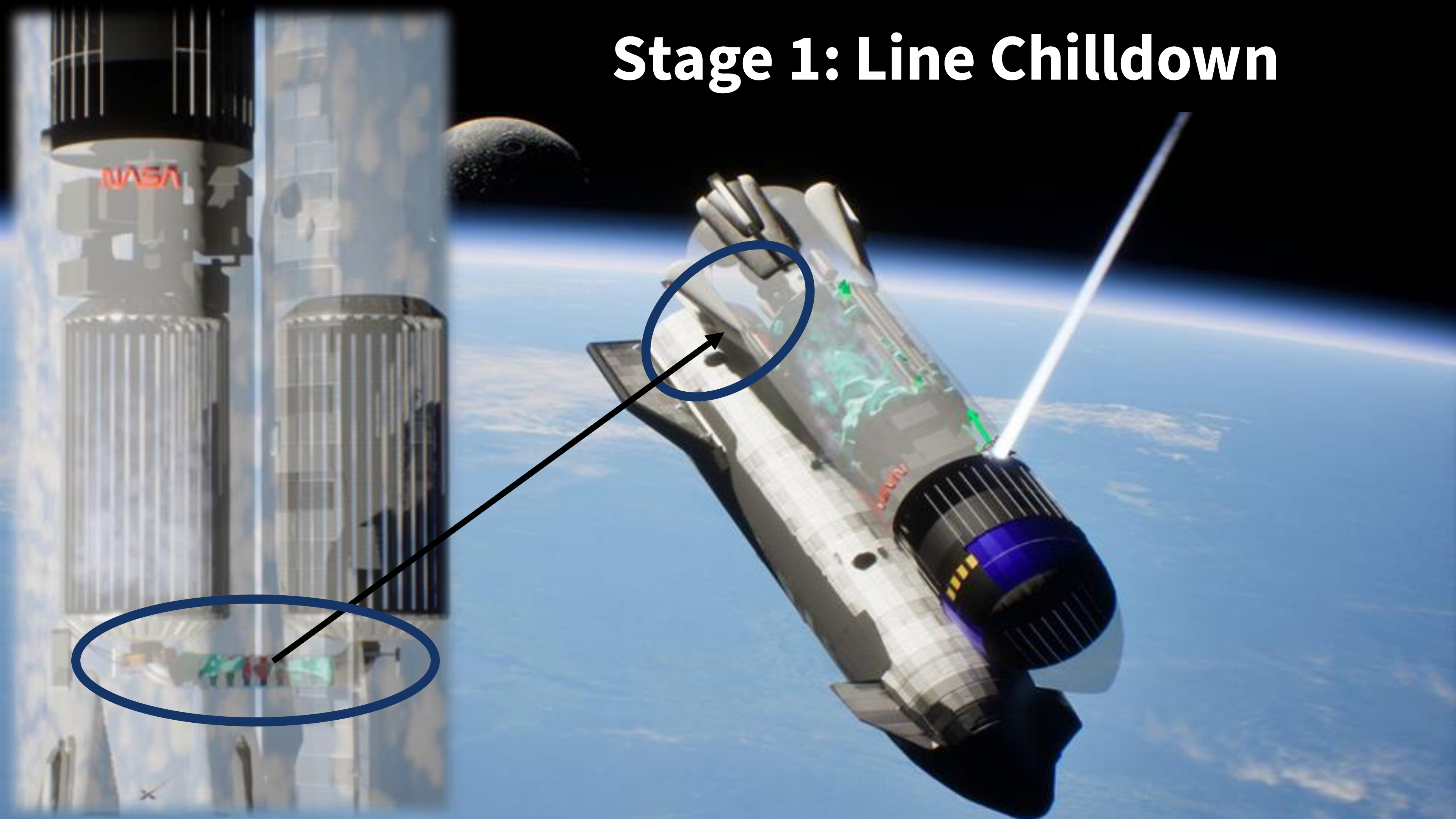

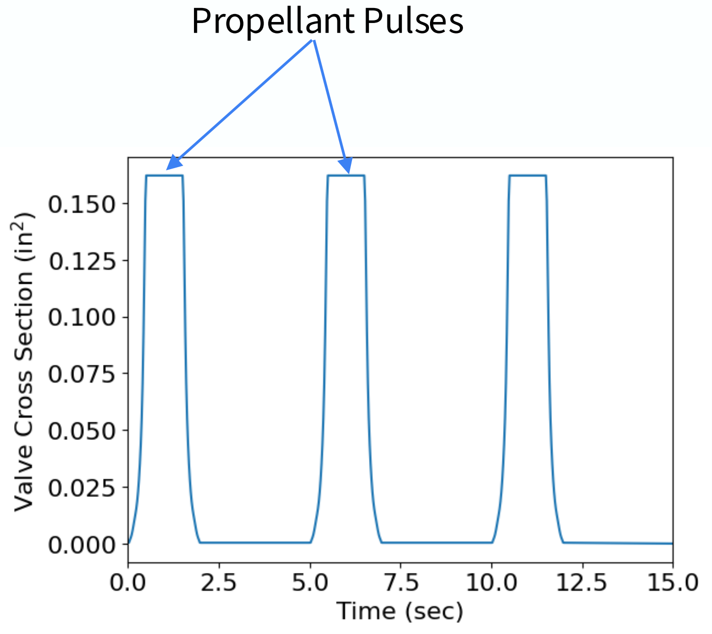

Pulsing propellant during line chilldown[1]

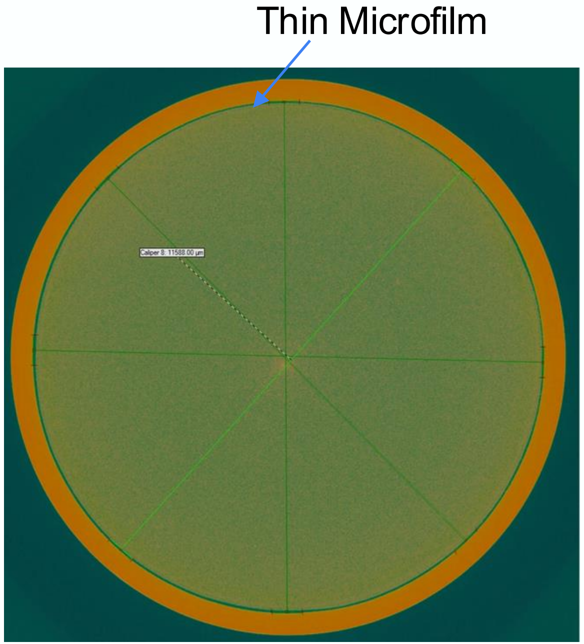

Pipe alterations[2]

Current research has focused on mass savings in the line chilldown process.

Pulse Flow Motivation

- Pulsed flow destabilizes its vapor film
- **Less consumed propellant mass** during line chilldown (compared to cont. flow)

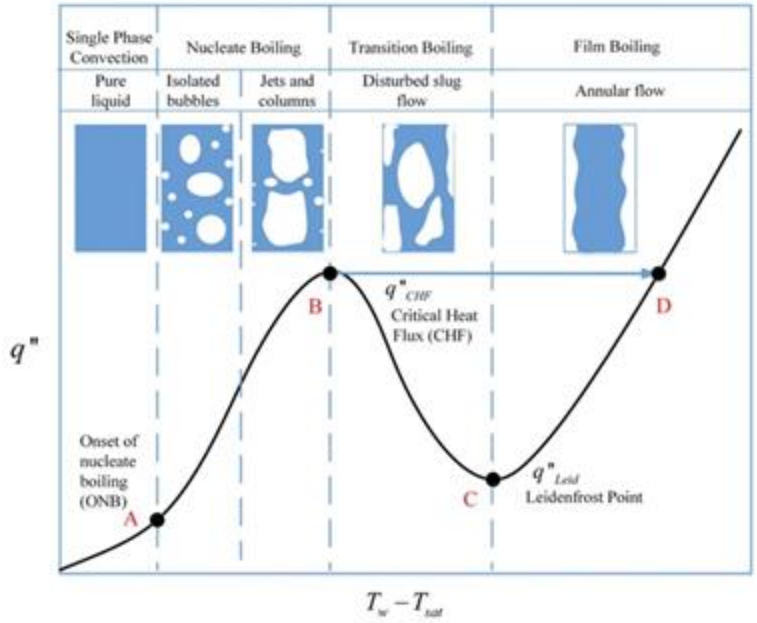

Flow boiling curve: film boiling insulates and reduces efficiency.

Pulse flow results in significant mass savings.

Pulse Flow Simulation

- Simulation developed based on existing literature
- Heat correlations obtained from Dr. LeClair.
- **Parameters**
  - 0.46in inner diameter
  - 0.02in pipe thickness
  - 22.5in pipe length
  - Fluid is LN2

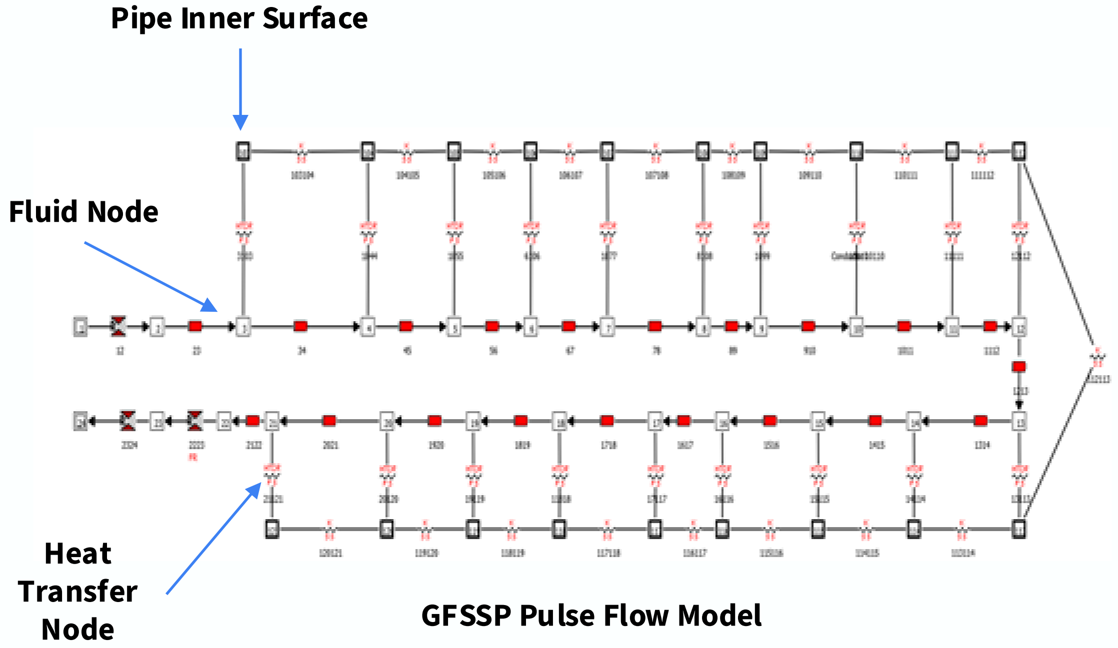

GFSSP Pulse Flow Model

GFSSP used to simulate pulsed flow.

Pulse Flow Simulation Results

- **Chilldown times**
  - Continuous flow: ~12 seconds
  - Pulse flow: ~ 20 seconds
- **LN2 Propellant Mass Used**
  - Pulsed flow saves up to **24% of propellant**
- Decreasing propellant mass utilized with higher valve close times

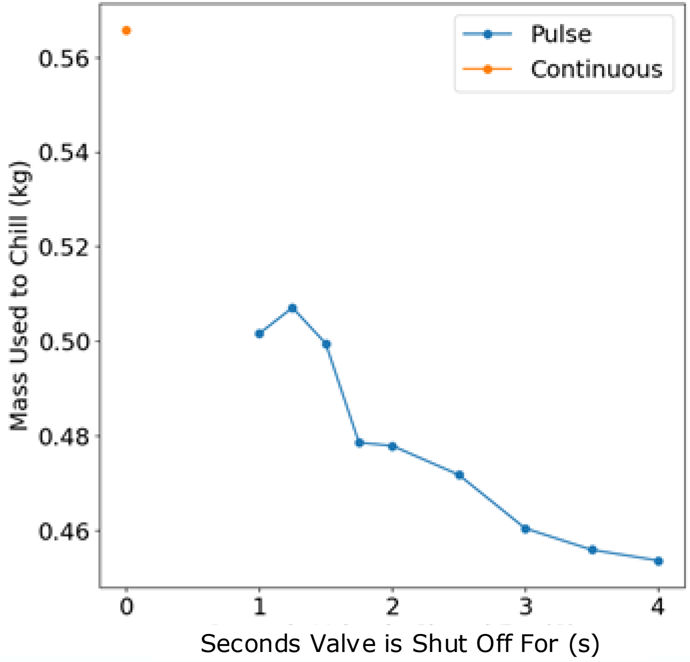

Propellant Mass Used to Achieve Chilldown for Different Valve Closed Times

Despite longer chilldown times, pulse flow results in significant mass savings.

Hydraulic Shock

- **Hydraulic shock effect:** Pressure spike that occurs due to rapid change in fluid momentum
- Lack of research within this field

- **Mitigation methods**
  - Increase pipe diameter
  - Decrease flow rate
  - Pressure spike damper
  - Increase valve closing times

- **This may reduce effectiveness of pulse flow**

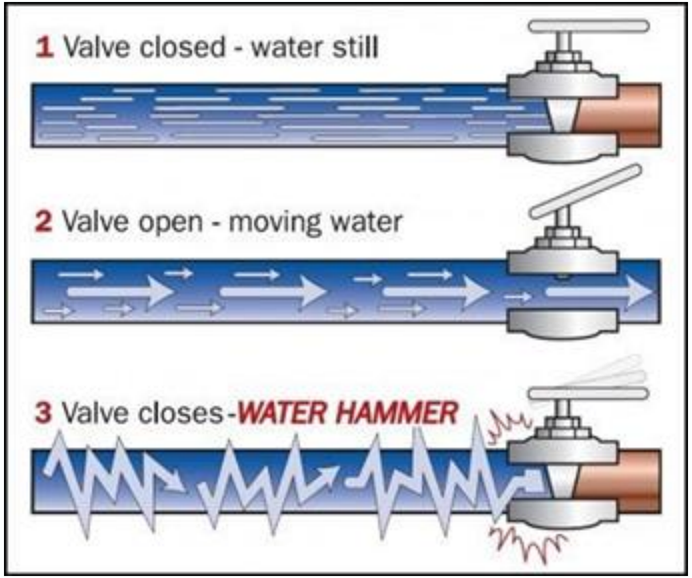

Water Hammer Progression[8]

Pulsed flow may induce the hydraulic shock effect, which can be reduced through optimal valve closing time.

Hydraulic Shock Simulation

- Model created using GFSSP
- **Parameters**
    - 127 psi – 87 psi
    - Total length : 60'
    - Pipe ID: 10"
    - Simulation tested for various open/close times

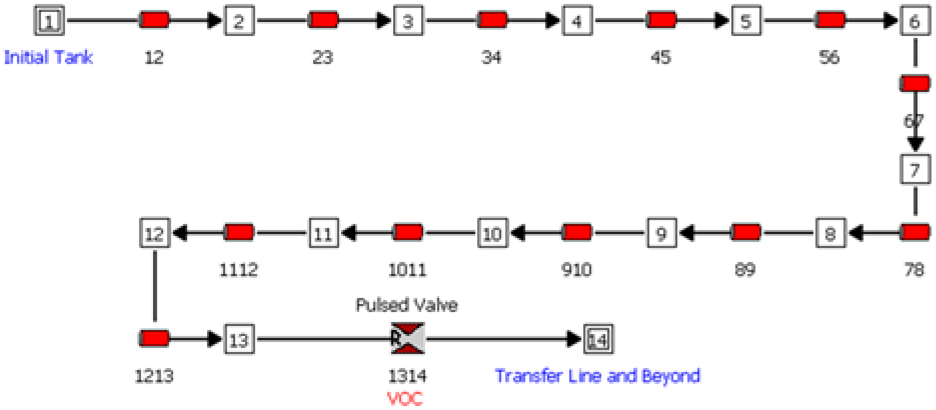

GFSSP Hydraulic Shock model

A safe valve closing time can be found to match an acceptable pressure spike.

Hydraulic Shock Simulation

- **ASME B31.4: max total pressure should not exceed 110% of design pressure**
- Valve limitations
  - Stronger motors/pneumatics may add mass/complexity
- Proposed open-close times
  - **Open:** as fast as possible
  - **Close:** two seconds or longer

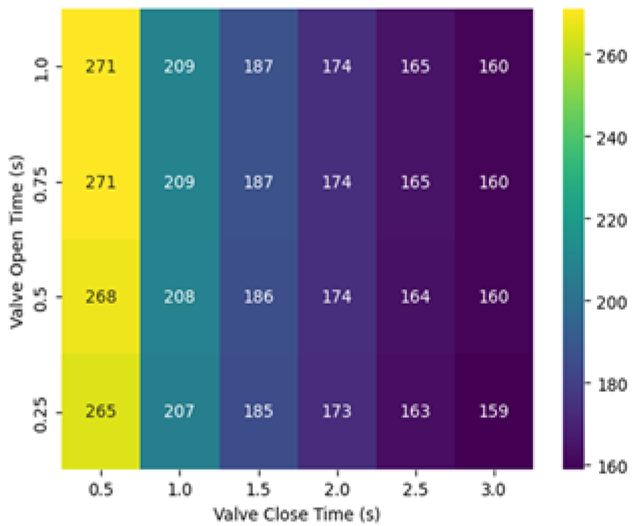

Maximum pressure in system as function of valve open and close time

Close time much more impactful than open time, hydraulic shock is a fixable issue

Tube Modifications and Coatings

- **Benefits**
  - Reduce boiloff during line chill-down
  - Increase heat transfer coefficient
  - Decrease chilldown time
  - Increase sensible latent heat
- Trade study conducted, microfilm chosen

Item	Microfilm Coating	Microfins	Capillary Coatings	Surface Etching	Microstructures	Weight
Technology Readiness Level	1	0.71	0.43	0.71	0.43	0.15
Manufacturing Readiness Level	1	0.5	0.25	0.5	0.375	0.15
Heat Transfer Enhancement	0.22	0.12	0.5	0.21	1	0.2
Pressure Fluctuation	0	1	0	0.48	0	-0.1
Durability	1	0.3	0.5	0.55	0.4	0.15
Total	0.494	0.1505	0.277	0.258	0.38075	

Modifying the tube's inner surface is an effective way to reduce propellant loss.

Tube Modifications and Coatings

- Low-conductivity coating insulates tube surface from bulk tube mass
  - Enables **faster film boiling**
- Optimal thickness balances initial cooling with ongoing heat conduction

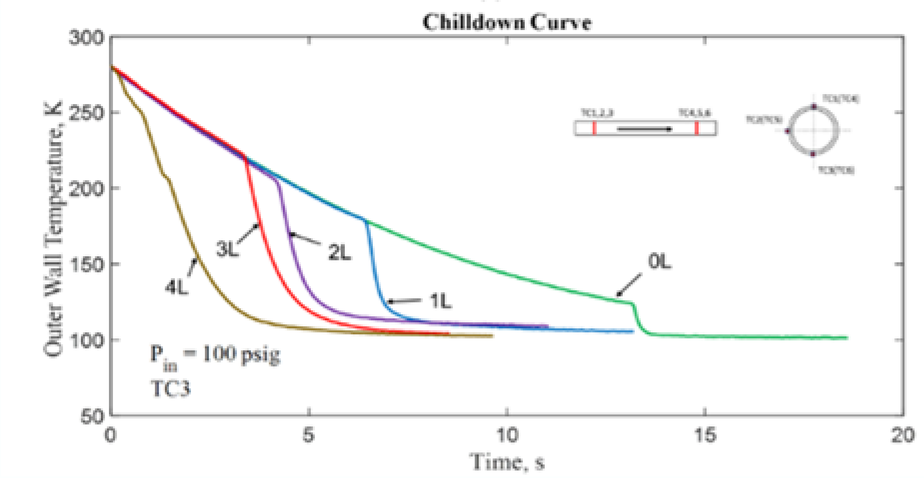

Chill-down curve with varying coating layers[16]

Low-conductivity microfilm coating enhances heat transfer, reducing the mass of propellant loss.

Tube Modifications and Coatings

Coating Material Options

- FEP: lower thermal expansion, more formable, used in more tests
- PTFE: wider temperature range, higher mechanical strength

Application Technique

- Pour and drain: used in experiments, can be inconsistent
- Spray coating: requires dedicated equipment, used in long tubes

Chosen: FEP with spray coating

The ideal microfilm coating is FEP applied to the tube using spray coating method.

Tube Modifications and Coatings

- Model created using GFSSP, based on existing literature
- Continuous flow utilized
- Modelled with Miropowlski heat correlations
- **Parameters**
  - 0.46in inner diameter
  - 0.02in pipe thickness
  - 22.5in pipe length
  - Fluid of LN2

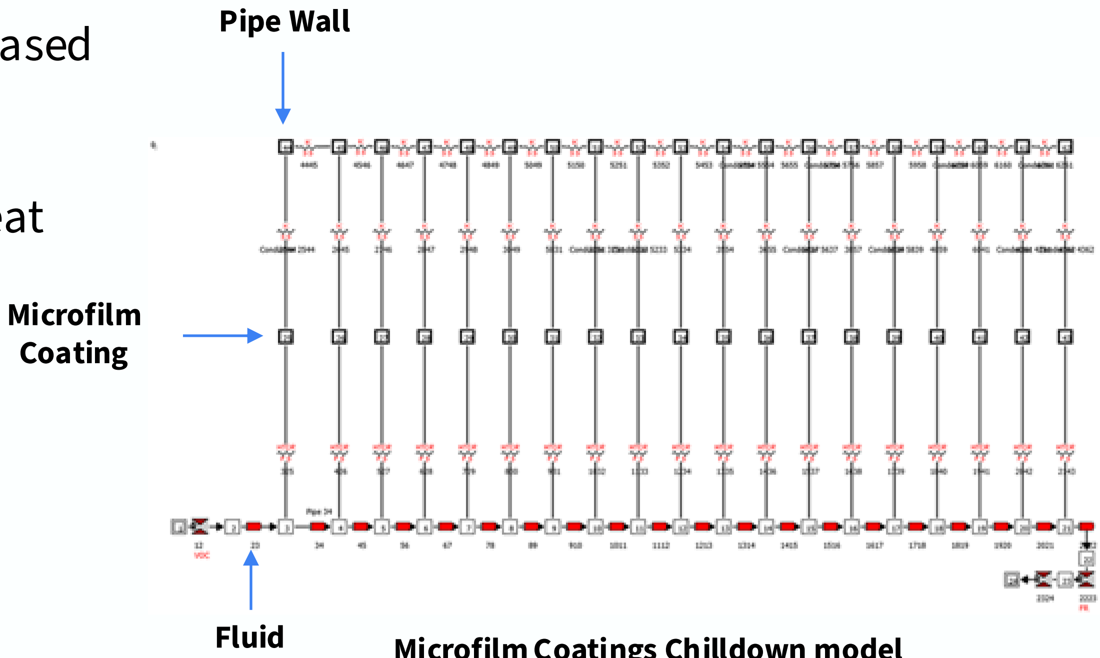

Microfilm Coatings Chilldown model

GFSSP can be used to simulate microfilm coatings effects on chill-down.

Tube Modifications and Coatings

- Microfilm model has **faster chilldown** due to higher heat transfer coefficient
- Allows for line to enter nucleate boiling regime **faster**

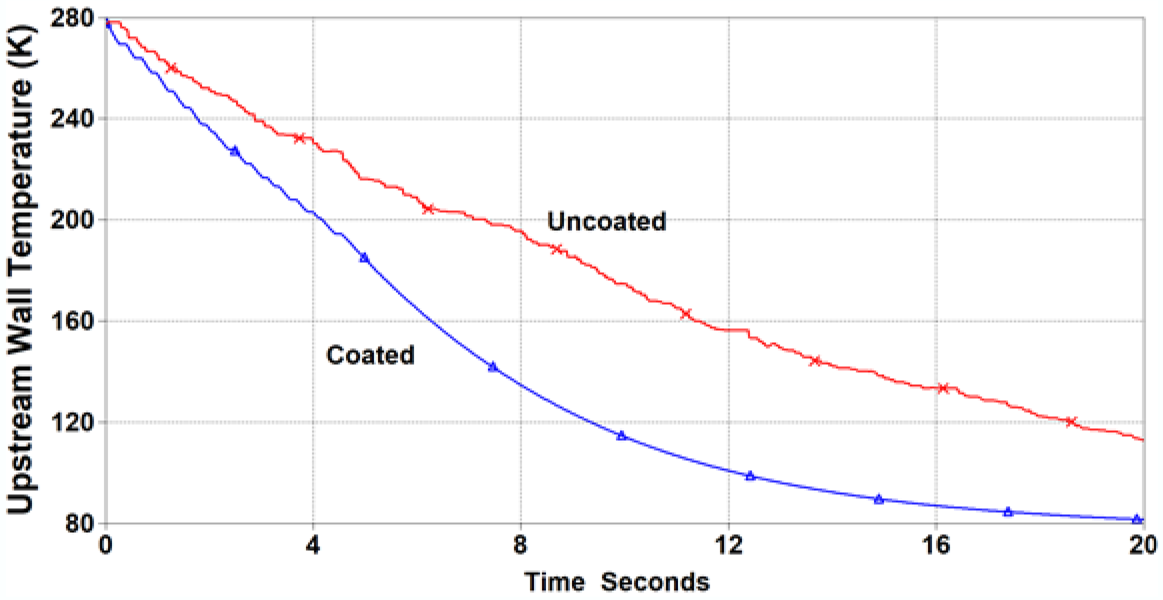

Upstream node temperature coated vs uncoated over time

Microfilm model results in faster line chilldown.

Key Innovations

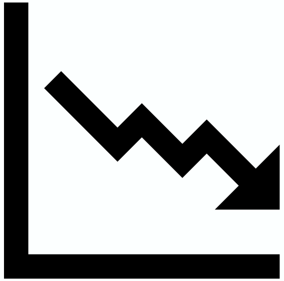

Pulse flow reduces propellant mass used

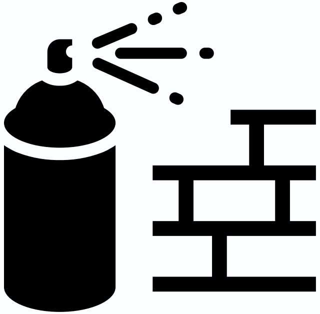

Microfilm coatings improve chilldown time

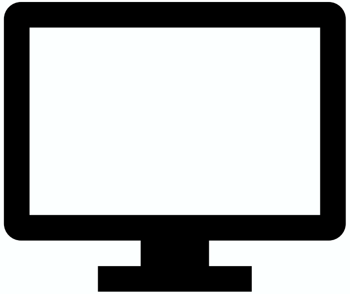

Solutions can be modelled through GFSSP

Stage 2: Tank Chilldown

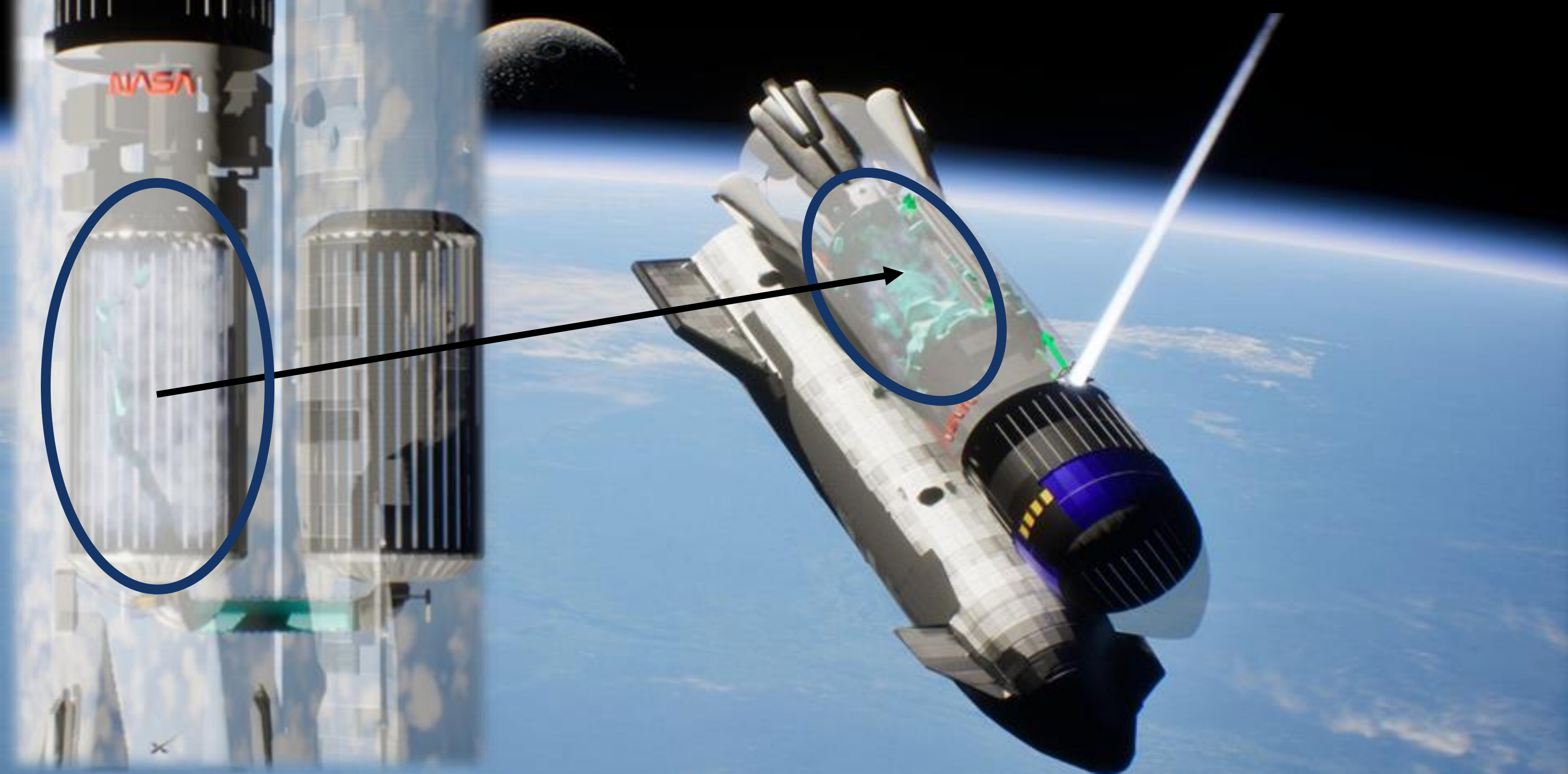

Motivation

- Key risks caused by microgravity environment
  - Tank over-pressurization
  - Accidental venting of ullage
- Priorities when performing tank chilldown
  - Lower propellant utilization
  - Maximize tank fill percentage
- **Solution: Charge-Hold-Vent (CHV) and No-Vent-Fill (NVF)**

Cryogenic tank chill fill is easier in gravity

Tank chilldown brings a risk of over-pressurization.

Charge Hold Vent & No Vent Fill

Steps:

1) Open and close valve to send a pulse of fluid
2) Allow fluid to completely boil while valve is closed, then vent gas
3) Repeat until tank is conditioned, then fill the tank without venting.

Benefits:

- Each charge is used efficiently
- No propellant is accidentally vented
- Tank over-pressurization risk is mitigated

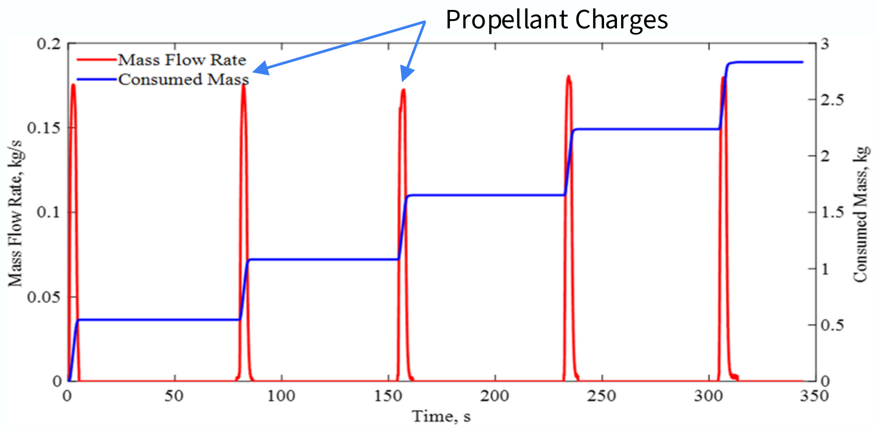

Cooling receiving tank with periodic propellant charges[3]

Charge Hold Vent (CHV) and No Vent Fill (NVF) mitigate over-pressurization while chilling down tank.

Tank Chilldown Transition

- Tank wall temperature is most consistent trigger to switch from CHV to NVF
- Place thermocouples at **areas of highest thermal mass**
  - Near structural interfaces like stainless-steel flanges

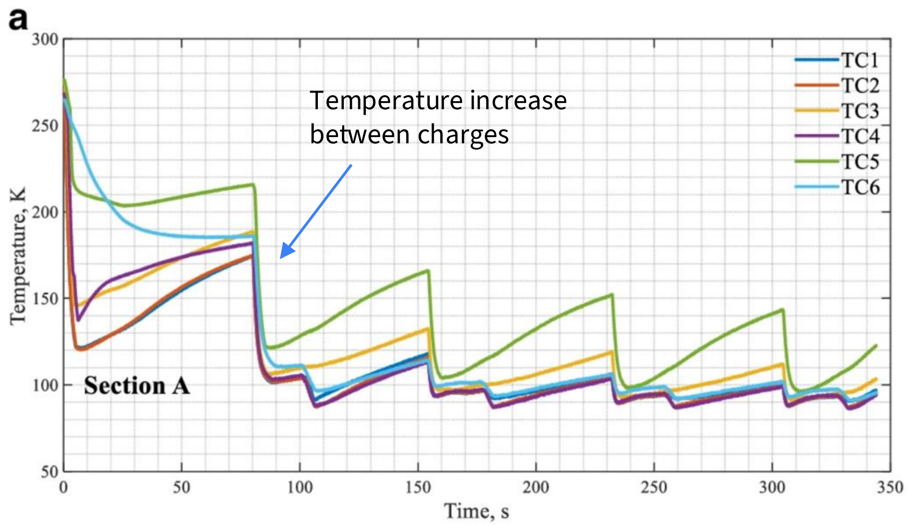

Highest thermal mass tank locations see largest temperature increase in between charges.

Transition point determined by areas with highest thermal mass.

Transition Point Calculation

- Script developed to solve for system
  - Stainless steel tank
  - 1200 m3 volume
  - 200 mT fluid transferred
- Final temperature = saturation temperature
- Output
  - Maximum Initial Temp for LOX = 105.35 K
  - Maximum Initial Temp for LHC4 = 129.61 K

$$m_{fluid,final}\,u_{fluid,final} - (m_{liquid,initial}u_{liquid,initial} + m_{vapor,initial}u_{vapor,initial}) - (m_{fluid,final} - m_{fluid,initial})h_{inlet} = \dot{Q}_{para,avg}\Delta t - m_{tank}\int_{T_{initial}}^{T_{final}} c_{tank}\,dT$$

Energy balance equation[21]

- Final fluid heat
- Initial fluid heat
- Heat gained from the inlet
- Loss to the environment
- Loss of the tank metal

- m = mass
- u = internal energy
- h = specific enthalpy
- Q = parasitic heat leak
- t = time
- T = temperature
- C = specific heat

An optimal tank temperature can be found to transition between CHV and NVF.

Key Innovations

Charge-Hold-Vent and No-Vent-Fill utilized

Hottest tank locations determine transition point

Optimal transition temperature can be determined

Phase 3: Propellant Transfer

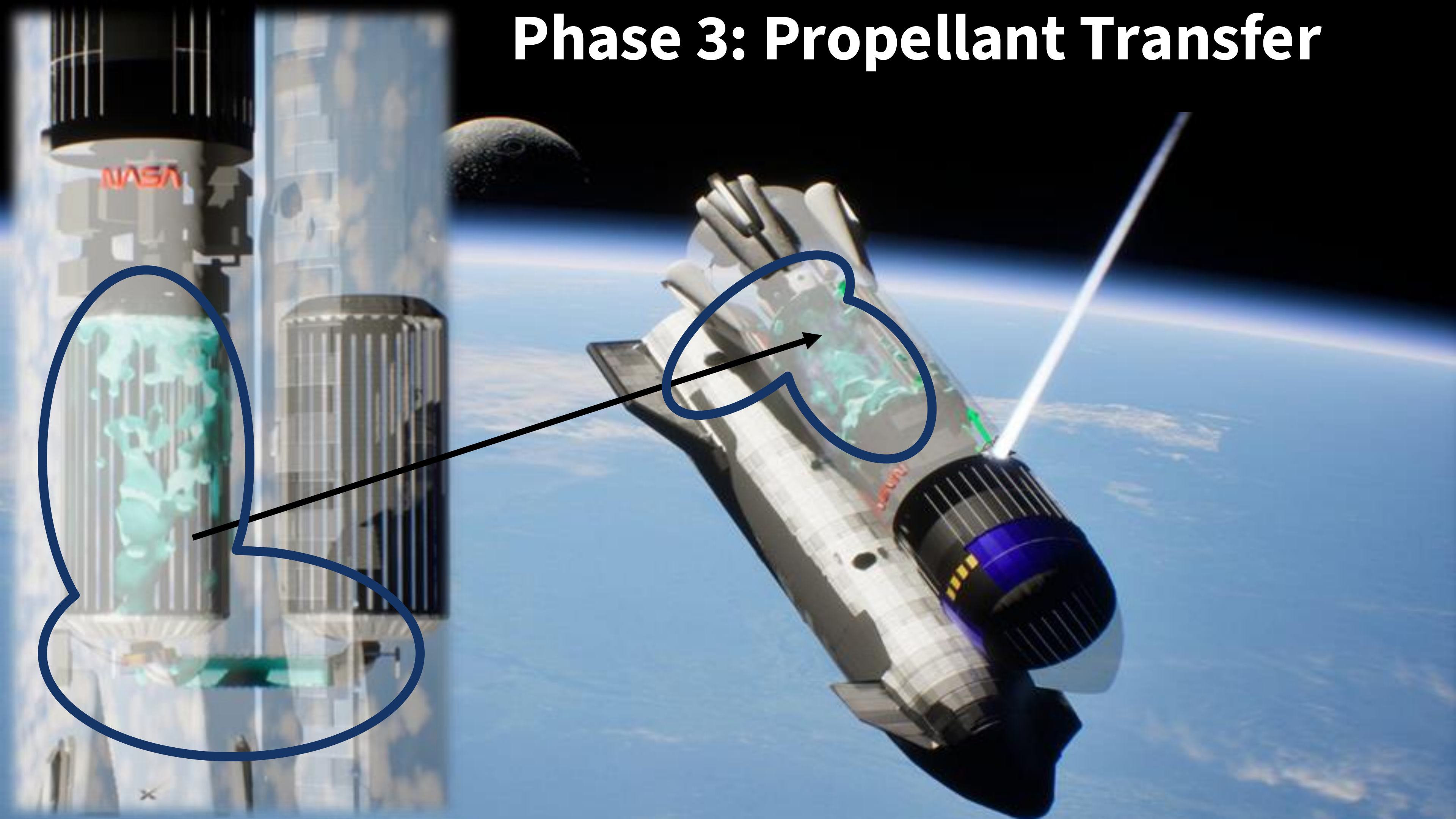

Flow Imaging Motivation

- Monitoring micro-g 2-phase flow regimes during transfer gauges transfer health
- Can point out:
  - **System heat leaks**
  - Propellant losses

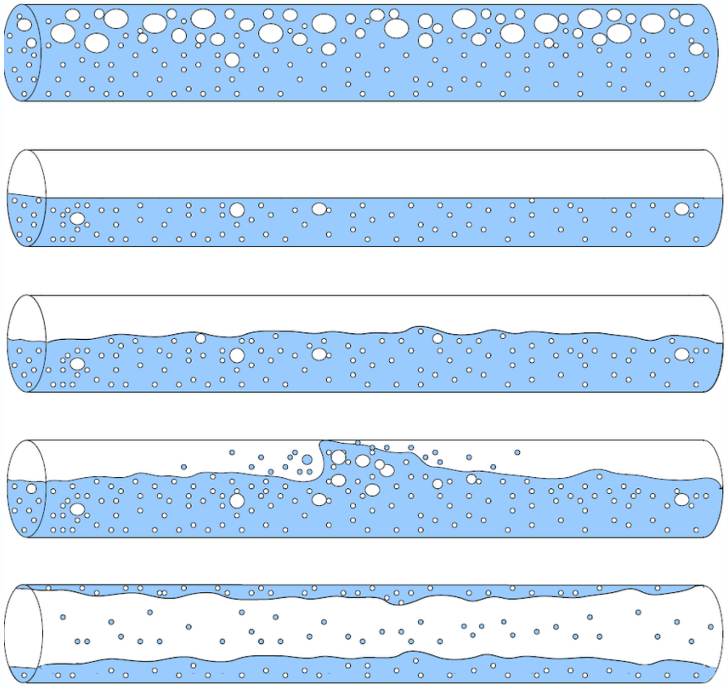

Flow patterns for 2-phase flow in horizontal pipes

State of the Art

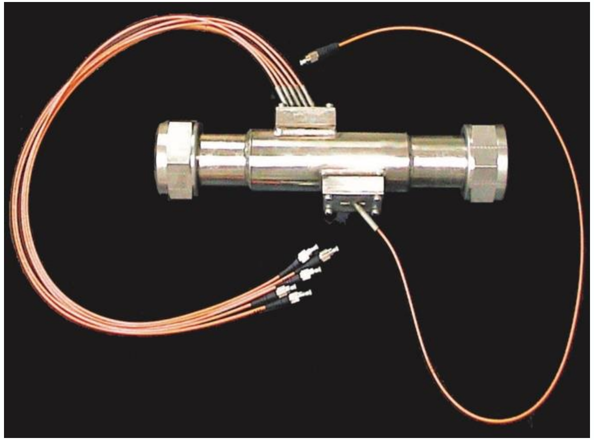

Fiber Optic Multi-Phase Sensor

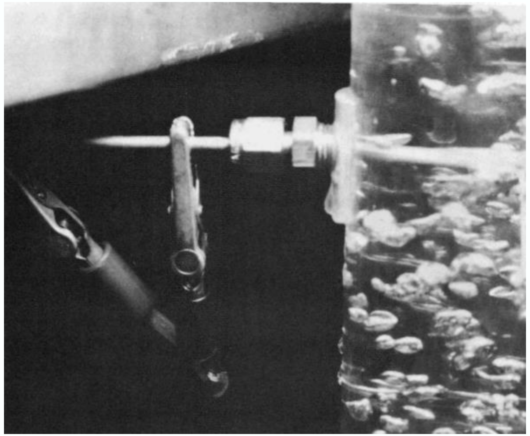

Electrical Resistivity Probe Sensor

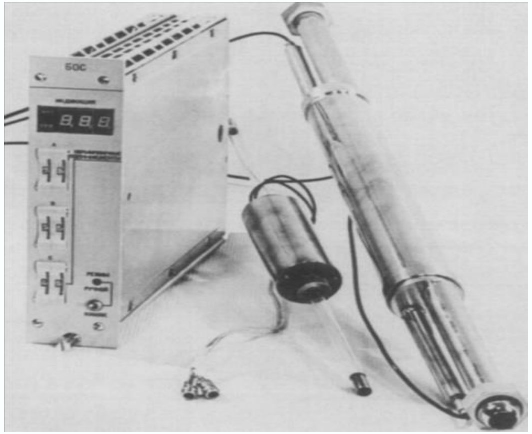

Radio Frequency Void Fraction Sensor

Current research is limited by unreliable measurements or system-level integration incompatibility.

Sensor Design Overview

Operation: Measures **time-domain capacitance** signal

Comprised of:

- Asymmetric Copper electrodes
- X-Aerogel insulation
- Aluminum sensor shield

Location: End of transfer Line

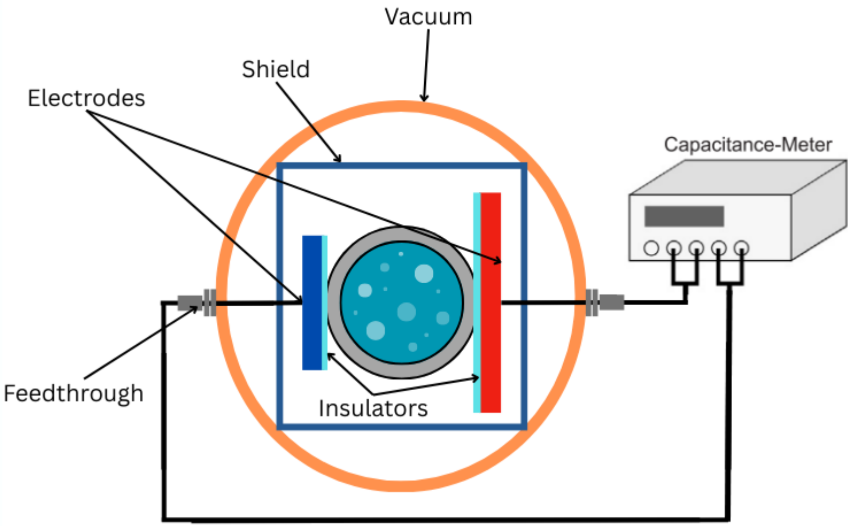

Capacitance 2-phase visualization

Why Capacitance Sensing?

- 2-phase flow sensing with a capacitance sensor is:
  - **Gravity independent**
  - **Minimally invasive**

- Measured time-domain capacitance signal is **informative about flow behavior**
  - Capacitance mean → void fraction
  - Statistical moments from signal → flow topology

$$\alpha_{linear} = \frac{C_L - C_M}{C_L - C_G} \times 100\%$$

Void fraction relationship with capacitance

C_L = Capacitance of the liquid

C_G = Capacitance of the gas

C_M = Measured capacitance

Sensor Requirements

Requirement	Value
Sampling Frequency	≥ 200 Hz
Excitation Frequency	10 Hz (Can burst to 1 kHz)
System Power	~ 10 W
Potential Difference	25 V

Sensor Calibration

- Calibration is done with Finite Element Method (FEM) simulations
  - Curve fit with void fraction vs capacitance trend
- Curve is verified using data from suborbital flights

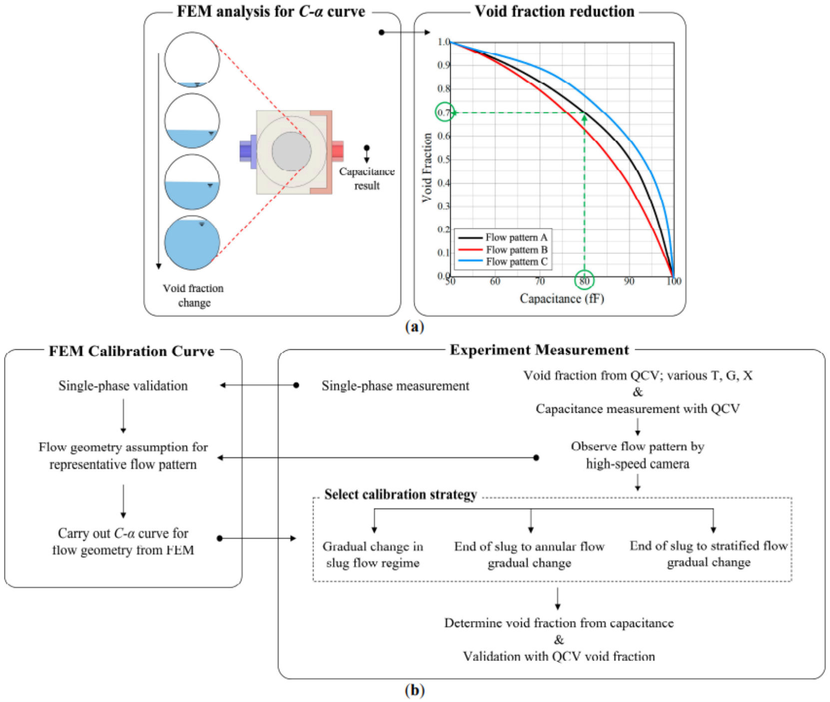

FEM analysis and proposed calibration process

Flow Regime Identification

Motivation: Monitoring two-phase flow regimes can identify

- **System Heat Leaks**
- Propellant Losses

Challenge: Past work coupled statistical features + Fourier Analysis for identification

- Fourier analysis requires **large datasets** for **coherent results**
  - Short micro-g test flights **limit datasets**

Goal: Develop flow regime identification technique using **time-domain statistical features** of measured capacitance signal

Flow Regime Map

- Flow regimes identified with
  - Mean (1st moment)
  - Variance (2nd moment)
  - Kurtosis (4th moment)
- **Probabilistic clustering** used to group points
- **High probability** of accurate flow regime detection
  - Smooth regime transitions

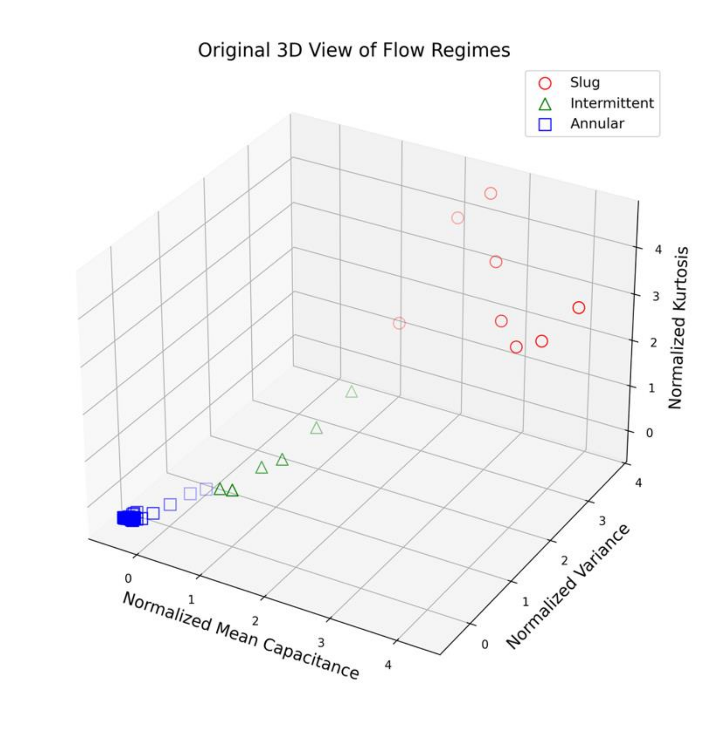

ECLIPSE Initial Flow Regime Map

Suborbital Concerns

- Two major concerns with micro-g experimental data
  1.) Duration of data
  2.) Imbalance of points per flow regime

- Extending data will overemphasize one flow regime due to **regime transitions**

- Solving (2) is much **more feasible**
  - Curve interpolation is done

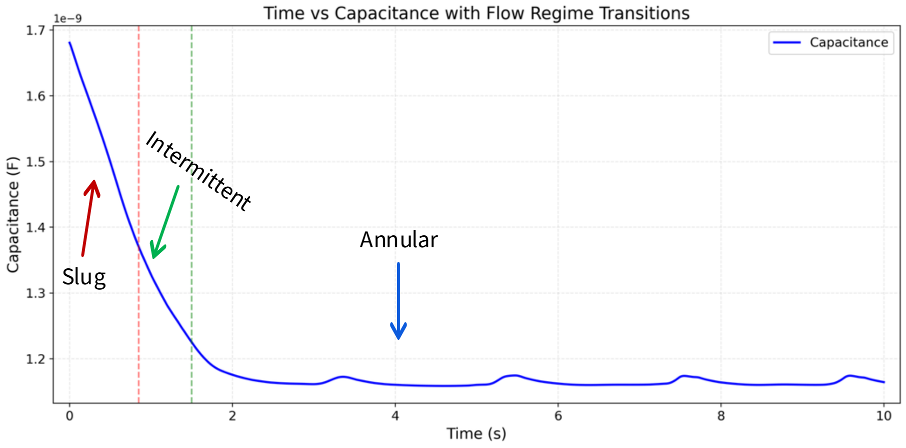

Measured Capacitance v Time from ANSYS

Curve interpolation

Curve interpolation done with **Gaussian Process Regression (GPR)**

- Machine Learning probabilistic interpolation model
  - Smooths out noise
  - Low probability of over-fitting

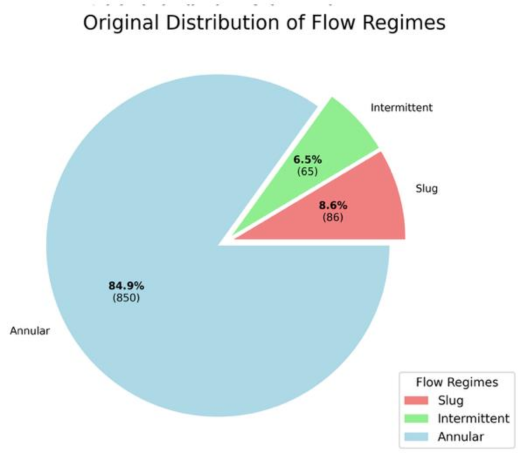

Before interpolation

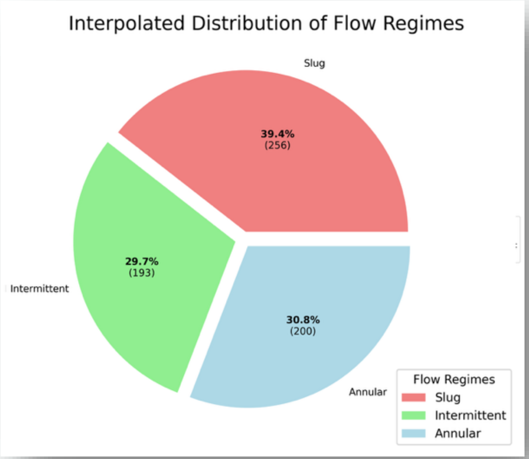

After interpolation

Final Flow Regime Map

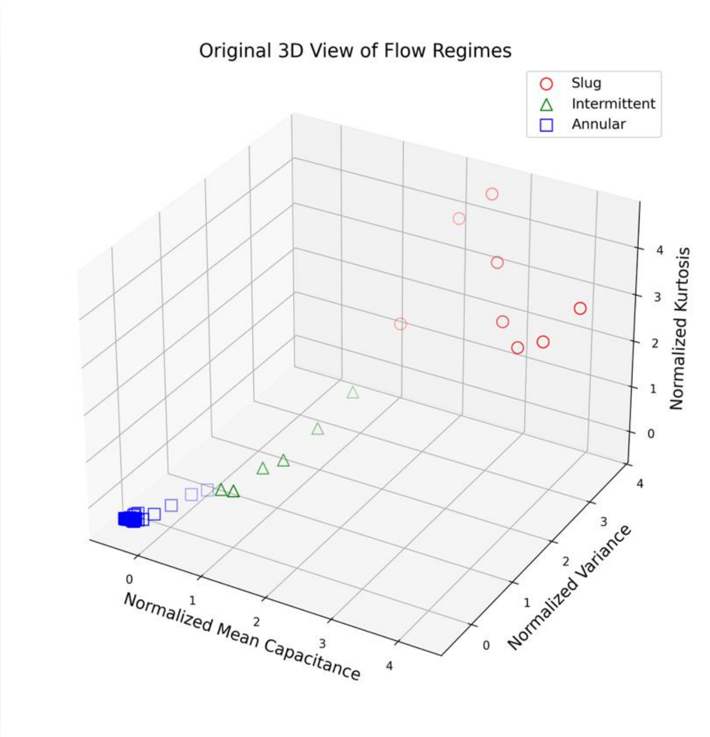

GPR

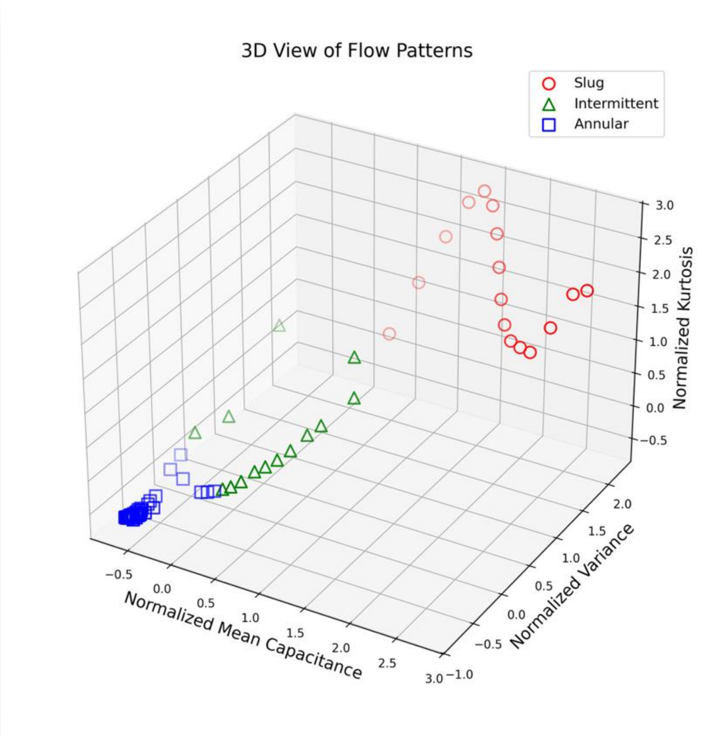

Key Innovations

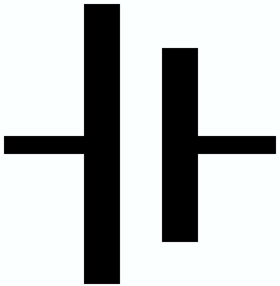

Capacitance sensor monitors propellant transfer health

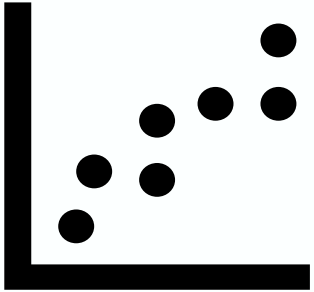

Statistical moments are used to determine flow regime

Propellant losses and heat leaks can be identified

Risk Informed Decision Making

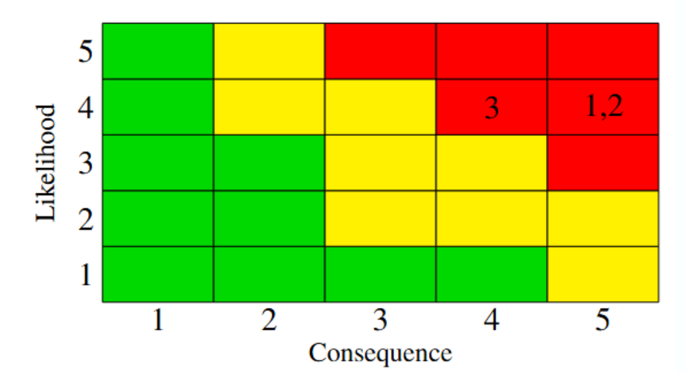

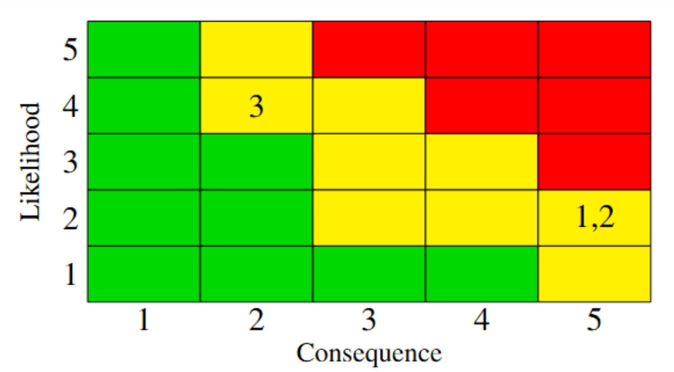

ID	Risk	Mitigation	Impact
1	Unvalidated microgravity fluid dynamics models	Conduct precursor flight experiments to calibrate micro-g models; integrate updates prior to final launch	Adjustments to current models and heat correlations
2	Valve depreciation from pulsed flow	Perform valve lifecycle testing under simulated pulsed flow conditions before system integration	Ensures robust chilldown protocol
3	Lack of funding	Conduct sensor feasibility and prototyping during ground test phase to reduce early-stage funding burden	Reduces development risk and keeps project on schedule

Ground & Prototype Testing

Suborbital & Parabolic Test Flights

Cost Analysis

- Two estimates were created used NASA Instrument Cost Model
  - Uses mass and power-driven cost estimation relationships (CERs) based on heritage instrument development
- **Lower bound:** $21.4 million
- **Higher bound**: $28.6 million

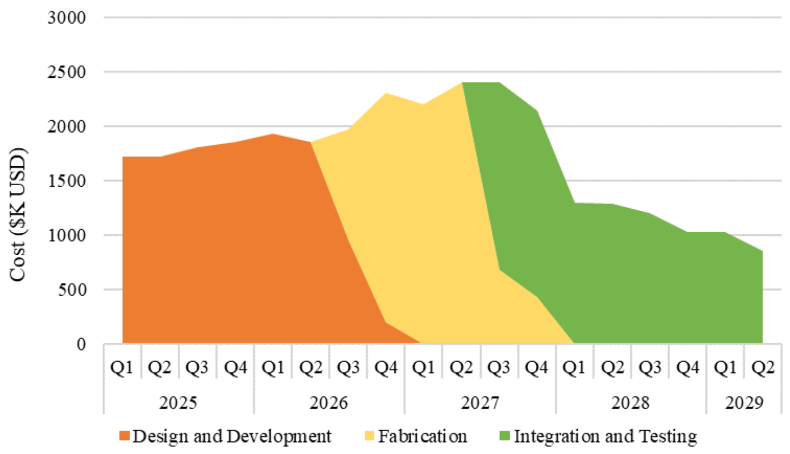

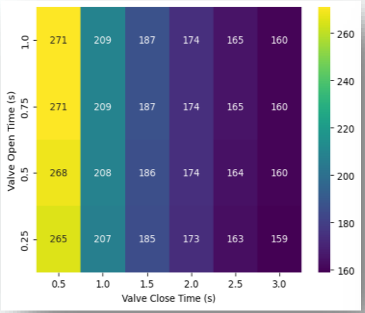

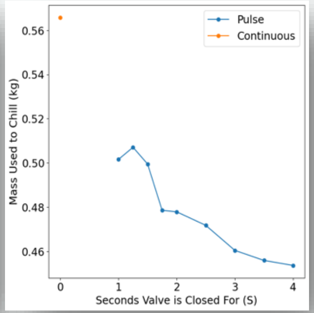

Proposed pulsed flow optimized with respect to heat efficiency and hydraulic shock

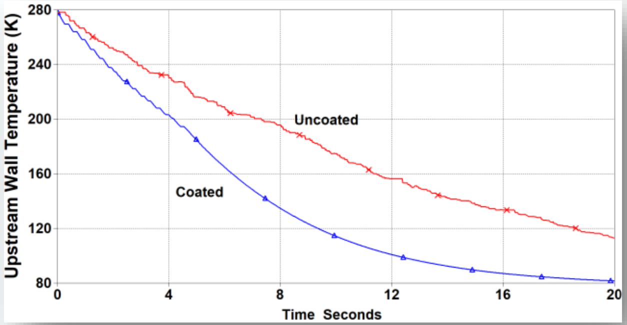

Developed a micro-film GFSSP modeling technique

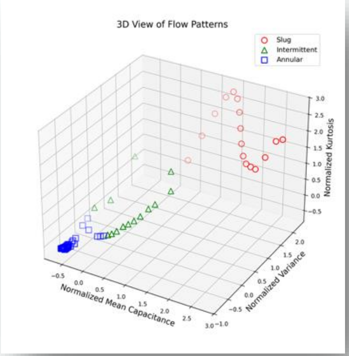

Created a novel 2-phase flow regime measurement technique

ECLIPSE

EFFICIENT CRYOGENIC LOW INVASIVE PROPELLANT SUPPLY EXCHANGE

2025 HuLC
HUMAN LANDER CHALLENGE

The Grainger College of Engineering
UNIVERSITY OF ILLINOIS URBANA-CHAMPAIGN

Faculty Advisor: Dr. Vishwanath Ganesan
Project Manager: Cliff Sun

Aneesh Ganti | Braedyn Kim | Charles Cundiff | Divij Garg
Robert Barthell | Thach Dang | John Galleta | Jett Haas
Keaton Jones | Justin Kotrba | Anna Lambros
Michael Milowski | Sebastian Moreno | Zahi Rahman
Sebastian Rojas | Anna Rudenko | Nate Vattana

Capacitance Sensor

Table 1

Dielectric constant of the materials used for the EFA simulations (* respective values [38]).

Material	State	ε	Material	State	ε
Nitrogen	Gas	1.000547	Hydrogen	Liquid	1.23
Oxygen	Gas	1.000494	Silicone oil	Liquid	2.17
Hydrogen	Gas	1.000272	Water	Liquid	80
Air	Gas	1.000536	PMMA	Solid	3.0
Nitrogen	Liquid	1.45	PTFE	Solid	2.1
Oxygen	Liquid	1.51	Alumina	Solid	9.9

$$C = \varepsilon_0 \varepsilon \frac{S}{d} [F]$$

$$\alpha_{linear} = \frac{C_L - C_M}{C_L - C_G} \times 100 [\%]$$

$$\alpha_{correct} = k\alpha_{linear}^2 + (1 - 100k)\alpha_{linear} [\%]$$

- S = electrodes surface area
- d = distance between the electrodes
- k = dimensionless number that depends on distance between electrodes

Sensor Components

Signal through vacuum:

- Hermetic Feedthroughs
  - Preserves vacuum integrity
  - Highly tested
  - Industry standard

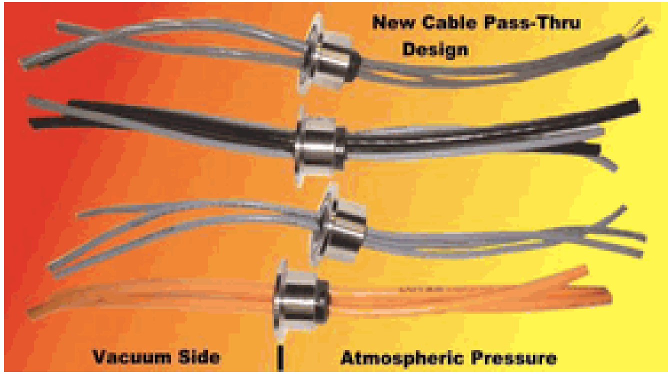

Insulator Material:

- Aerogel Insulator (X-aerogel)
  - Ultra-lightweight
  - Effective thermal & electrical insulators
  - Previously implemented in space

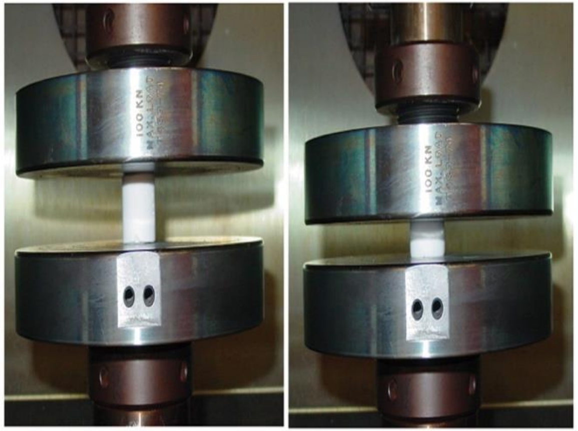

Sensor Geometry

- Asymmetrical
  - Reduced electric field curvature compared to other geometries
  - Higher accuracy because of stronger correlation between EFA and experimental capacitance-void fraction measurements

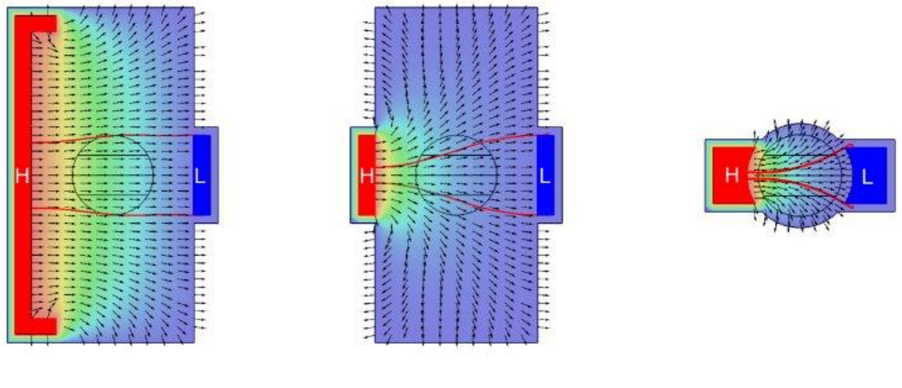

(a)Asymmetrical (b)Flat (c)Concave

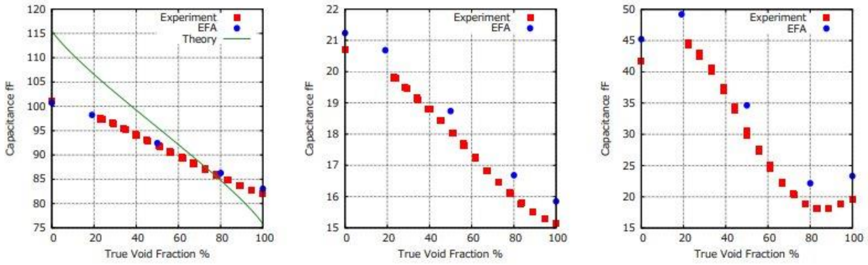

(a)Asymmetrical (b)Flat (c)Concave

Asymmetrical capacitance sensor leads to higher accuracy

Sensor Geometry Models

CAD models comparing each sensor type

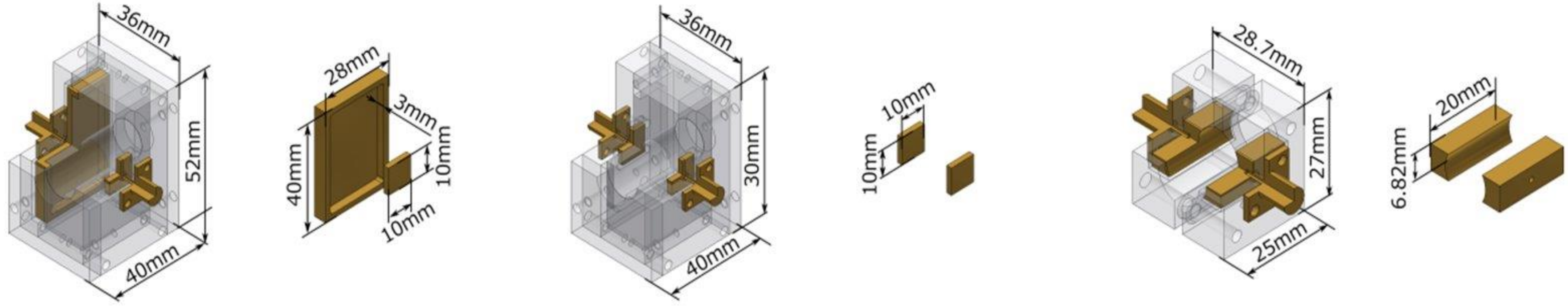

(a)Asymmetrical (b)Flat (c)Concave

"Thermal Effect" Correction

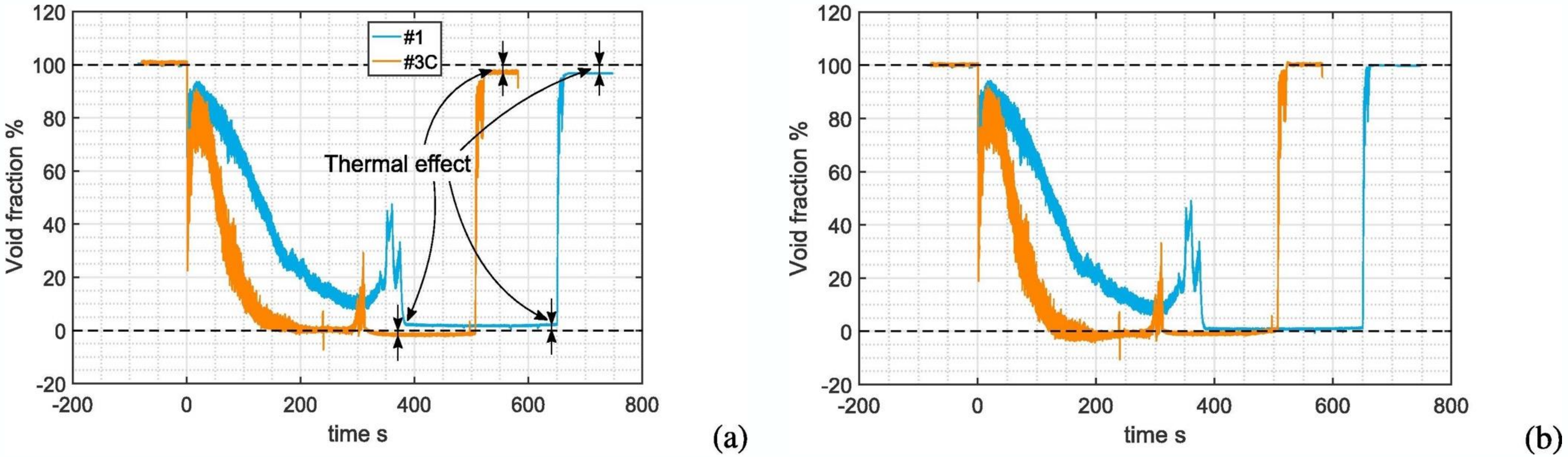

Fig. 9. Test #1 and Test #3C void fraction time histories before (a) and after (b) the "thermal effect" correction.

Accounting for thermal component shrinkage with new equations

FEM Simulations

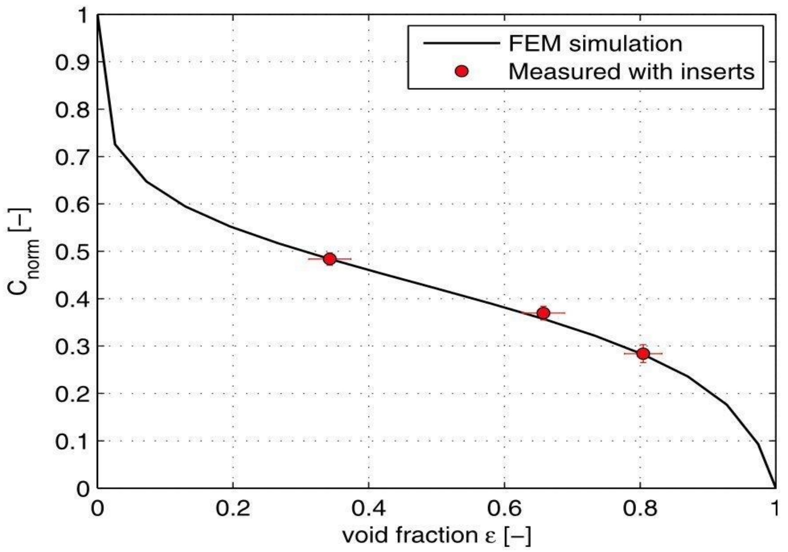

Fig. 3. Comparison of the capacitances measured for the inserts and the ones predicted by the FEM simulation.

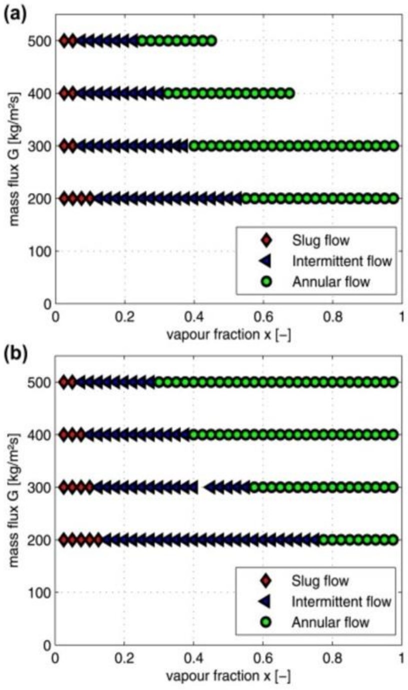

Download: Download full-size image

Fig. 5. Result of the flow mapping technique of Canière et al. [12] for the used dataset (a) R134a (b) R410A.

$$\varepsilon_{\text{intermittent}} = \frac{(1 - F95) \cdot \mu \cdot \sigma \cdot \varepsilon_{\text{slug}} + (1 - \mu) \cdot (1 - \sigma) \cdot F95 \cdot \varepsilon_{\text{annular}}}{(1 - F95) \cdot \mu \cdot \sigma + (1 - \mu) \cdot (1 - \sigma) \cdot F95} \tag{2}$$

Insulator Materials Trade Matrix

Material	Ceramic Fiber	Alumina	Aerogel	X-Aerogel
Cost ($/lb)	12.64	5.93	23,000	18,000
Density (kg/m^3)	96	3600	0.075	50
Thermal Insulation (R-value)	3.75	12	10.3	20
Dielectric constant	3.55	9.4	1	1.4
Compressive Strength (PSI)	78	296,000	23	30,000
MRL	10	10	9	6

Unweighted

Criterion	Weight	Ceramic Fiber	Alumina	Aerogel	X-Aerogel
Cost	-0.10	0.0005	0.0002	1	0.78
Density	-0.10	0.027	1	0.00002	0.014
Thermal Insulation	0.20	0.18	0.6	0.52	1
Dielectric Constant	-0.10	0.38	1	0.11	0.15
Compressive Strength	0.15	0.0002	1	0.00007	0.10
MRL	0.10	1	1	0.9	0.6
Total		**0.0952**	**0.170**	**0.0830**	**0.1806**

Weighted

Shield Materials Trade Matrix

Criterion	Aluminum	Copper
Cost ($/lb)	1.12	4.32
Density (kg m^{-3})	2 700	8 920
Skin Depth @ 1 MHz (μm)	82	65
Electrical Conductivity (% IACS)	59	100
Specific Strength (MPa·cm^3/g)	115	25
Corrosion Rating (1–10)	8	6
Machinability Index (% B1112)	270	20

Unweighted

Criterion	Weight	Aluminum	Copper
Cost	-0.12	0.26	1.00
Density	-0.14	0.30	1.00
Skin Depth	-0.20	1.00	0.79
Electrical Conductivity	0.35	0.59	1.00
Specific Strength	0.15	1.00	0.22
Corrosion Rating	0.10	1.00	0.75
Machinability Index	0.10	1.00	0.07
Total		**0.283**	**0.047**

Weighted

Mesh Configuration

- **227,561 nodes / 971,603** (near student license limit)
- Swept mesh with free-seed face (quadrilateral/triangular elements extruded axially)
- No inflation layers but adaptable for future wall resolution improvements.

Solver & Model Settings

- Transient pressure-based solver (Eulerian multiphase model)
- Phases: **Oxygen gas** (primary) / **liquid oxygen** (secondary)
- Lee model for phase change (evaporation/condensation)
- SST k-omega turbulence model with mixture properties.

Material Properties

- Liquid/gaseous oxygen properties sourced from ANSYS database.
- Future preference: Model oxygen gas as **incompressible ideal gas** for operational realism.

ANSYS Simulation Framework

Boundary Conditions

- No-slip walls / Velocity inlet (liquid oxygen: 1 m/s, 300 K)
- Liquid oxygen inlet volume fraction: 1 (pure liquid entry)
- Aluminum pipe walls with **0 W/m^2 heat flux** (adiabatic).

Solution Controls & Outputs

- Time step: **0.01 s** / Total steps: 990 (adjustable for transient resolution)
- Outputs: **Phase volume fraction** data, fluid domain axis animations.

Key Note

- Framework designed for future upgrades (pressure inlet, heat transfer analysis)

Flow Regime Map Slices

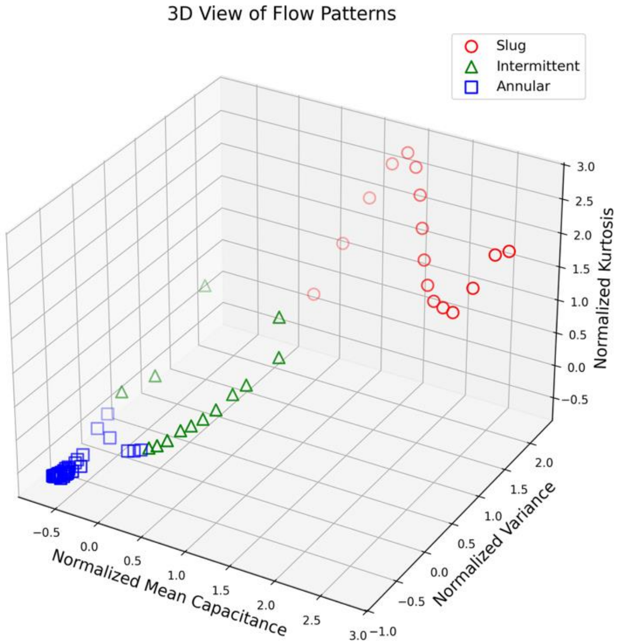

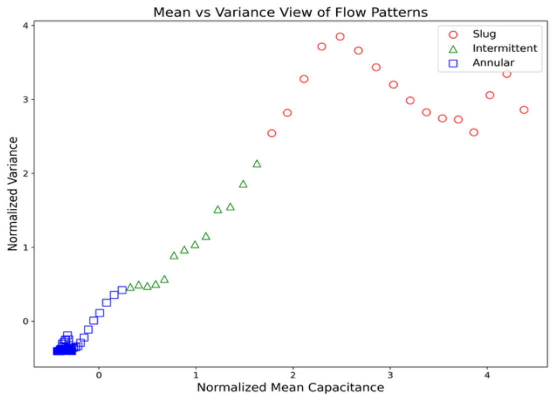

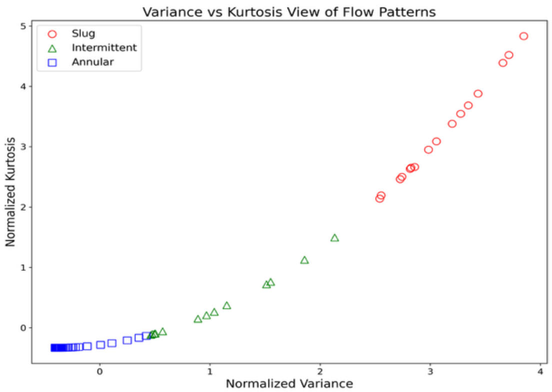

Flow Regime Wrap-up

- Three statistical parameters (mean, variance, and kurtosis) distinguish different flow regimes

- Interpolate data using Gaussian Process Regression for even distribution of points per flow regime

Enables: Real time flow regime identification by matching measured parameters using map

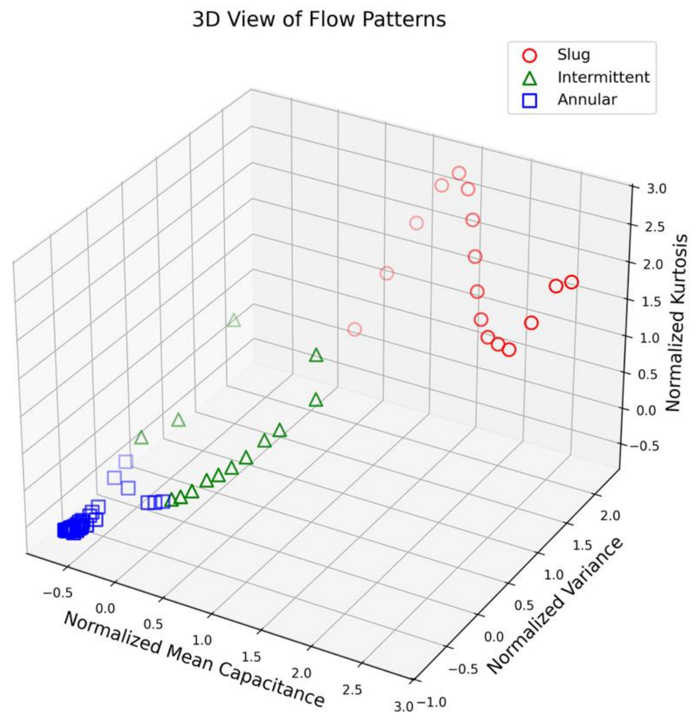

GFSSP Model Comparison

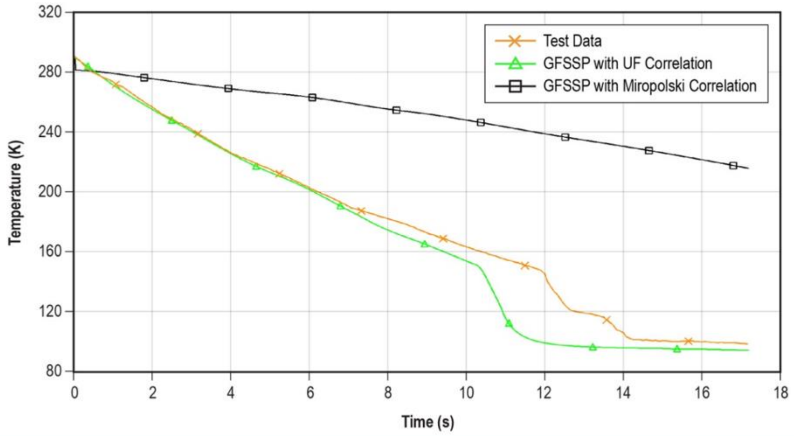

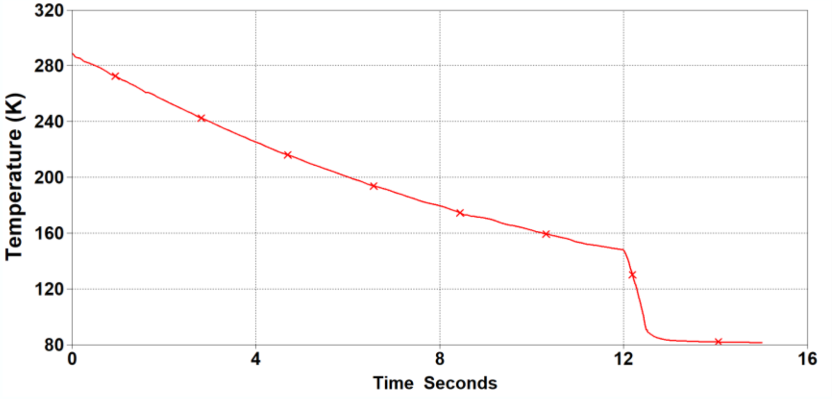

Mean Re ~68000 and Mean Re 41000

Zero-G Simulation Continuous

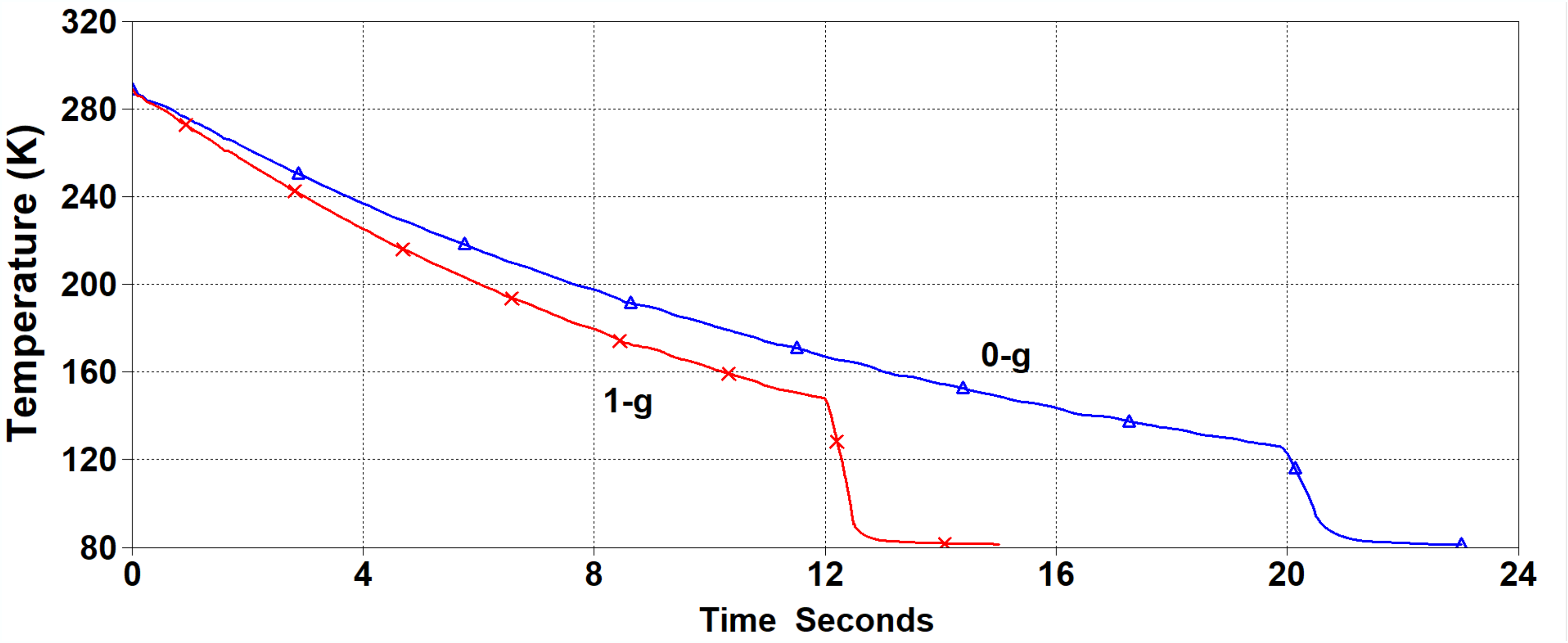

Zero-G Simulation Pulse

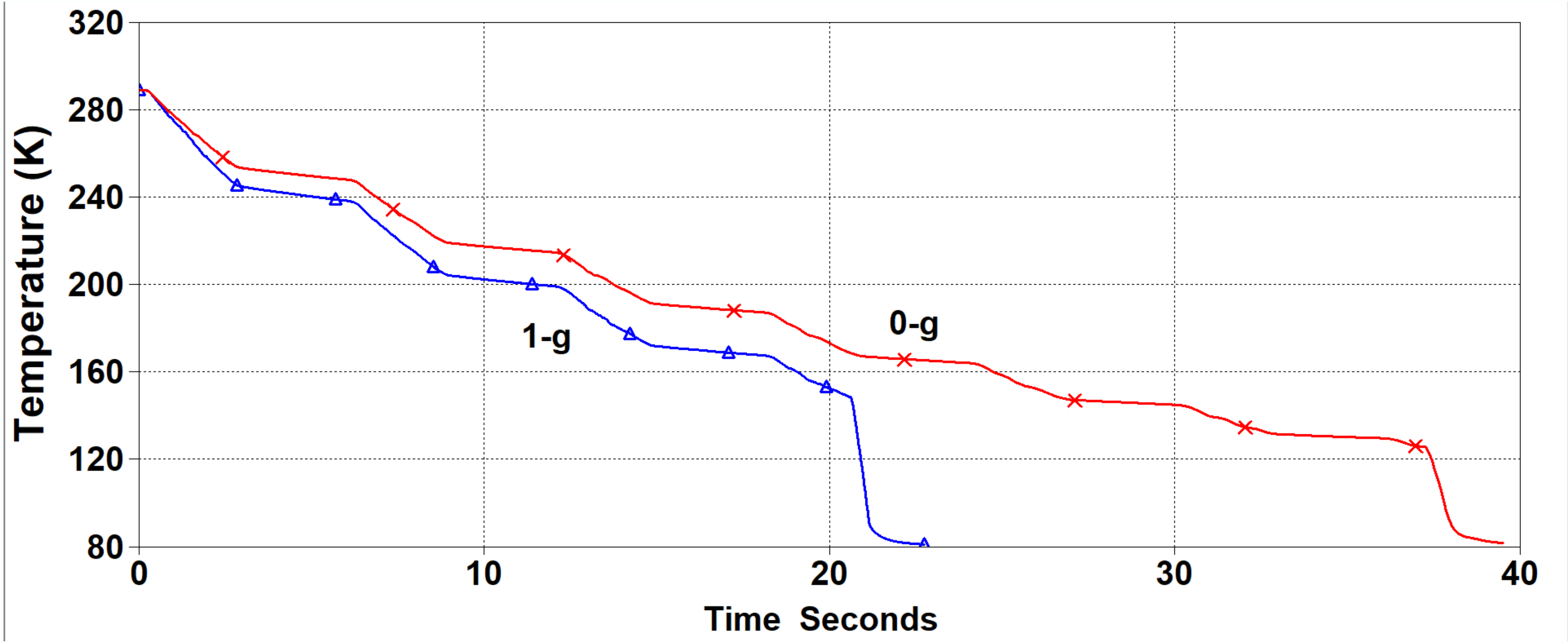

Continuous Flow Upstream

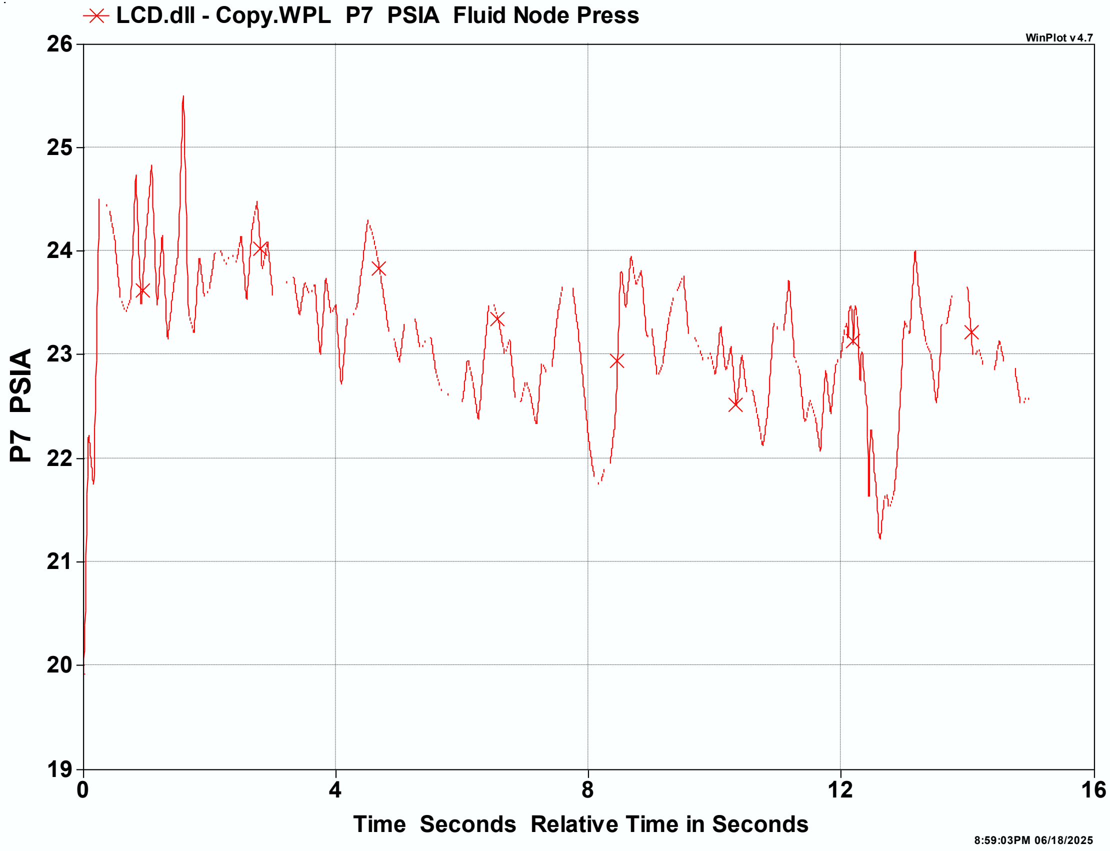

Pulse Flow Upstream

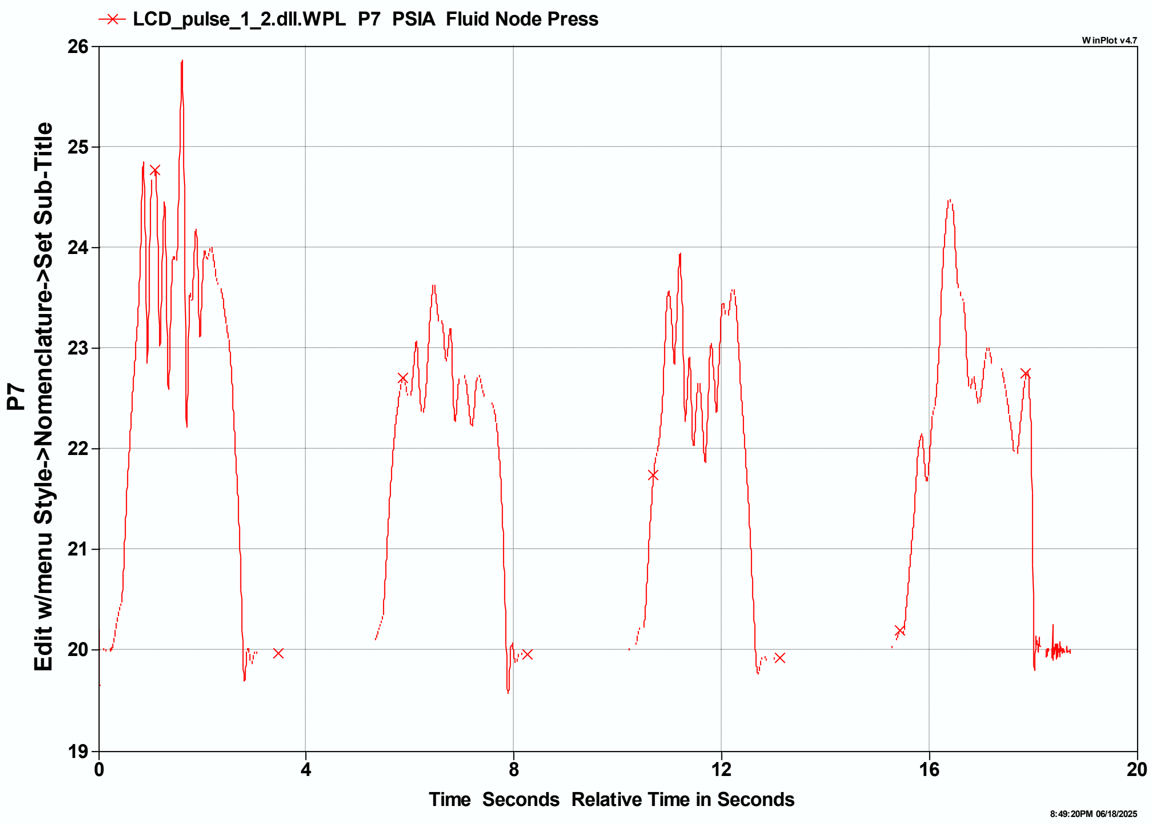

Microfilm Upstream

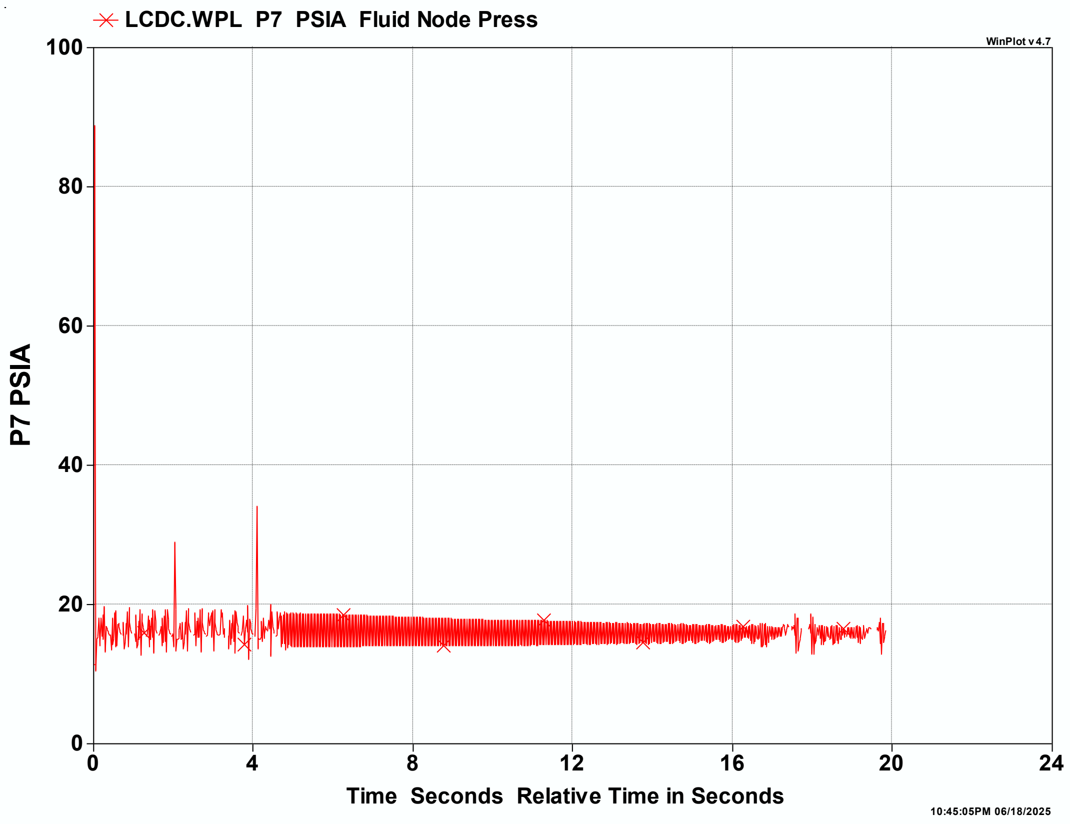

Continuous Flow Upstream

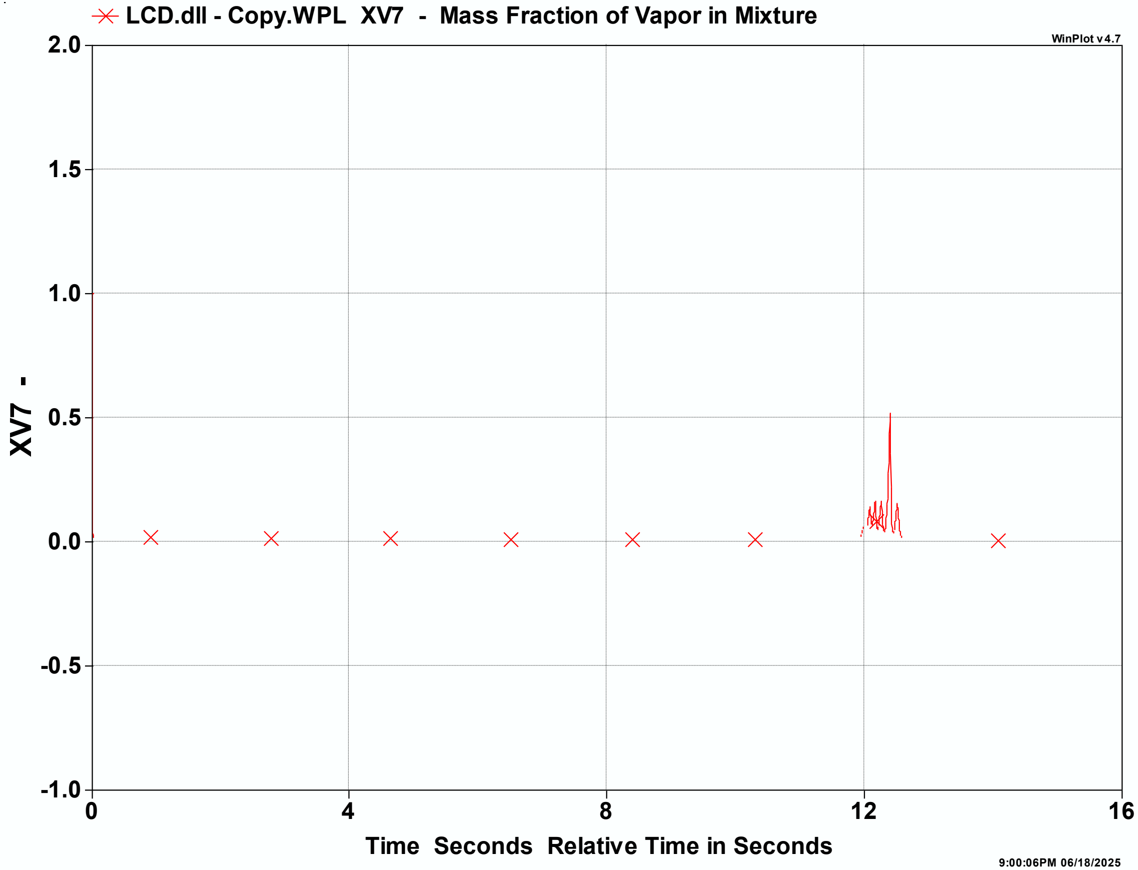

Pulse Flow Upstream

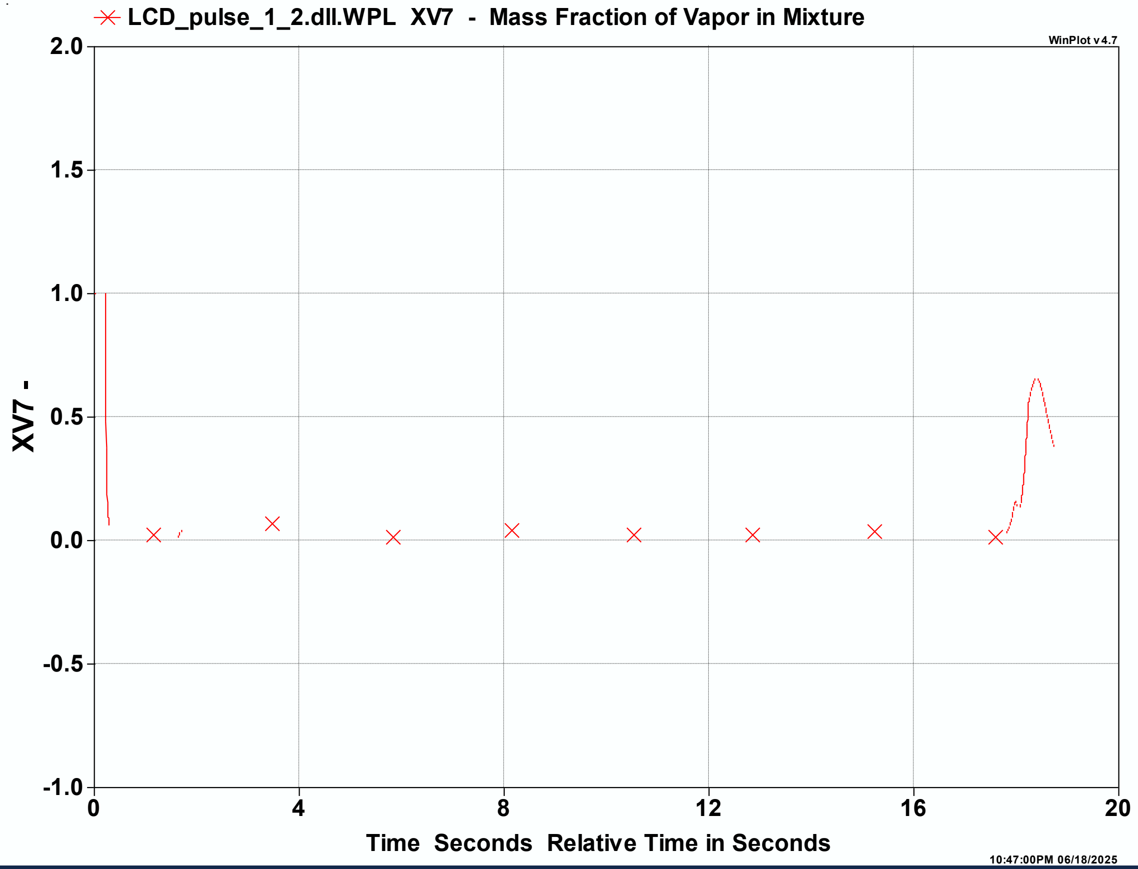

Microfilm Upstream

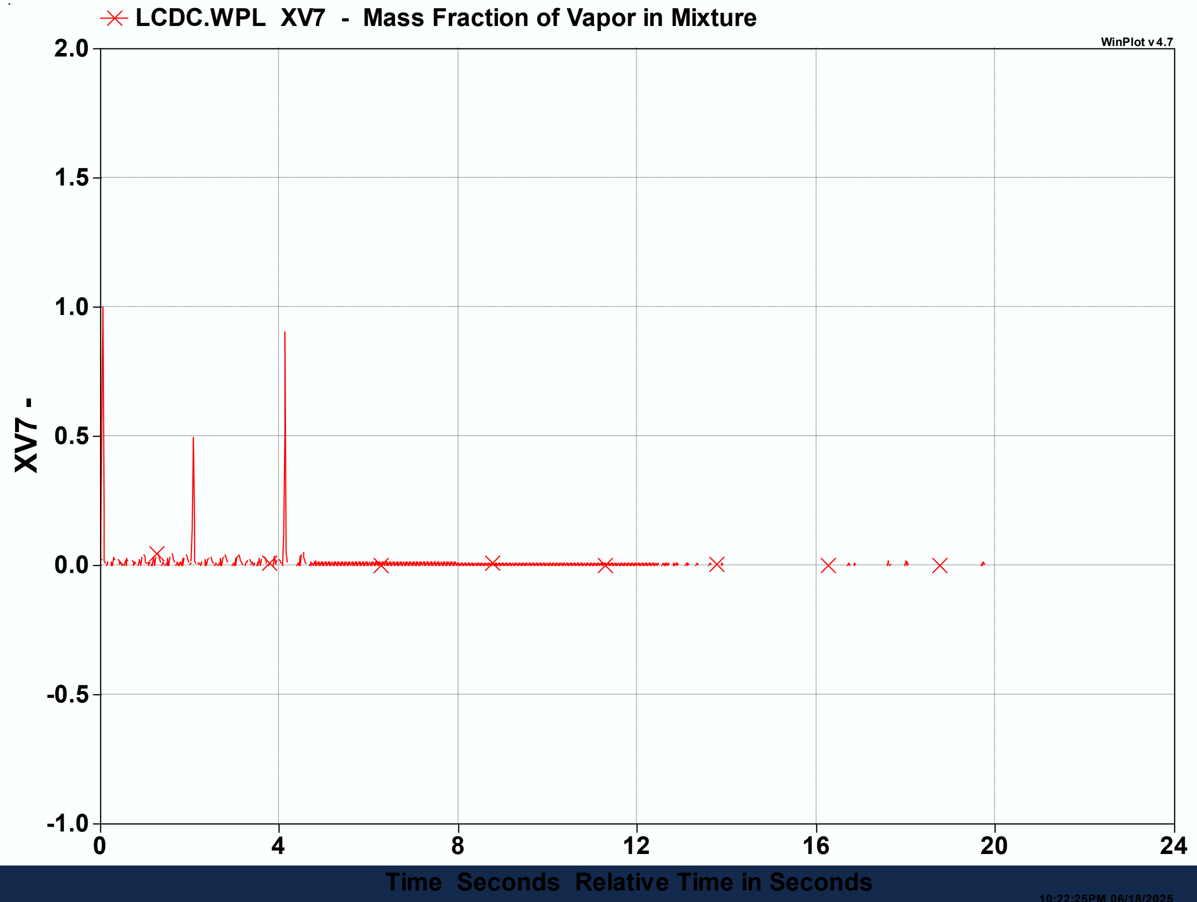

Continuous Flow Upstream

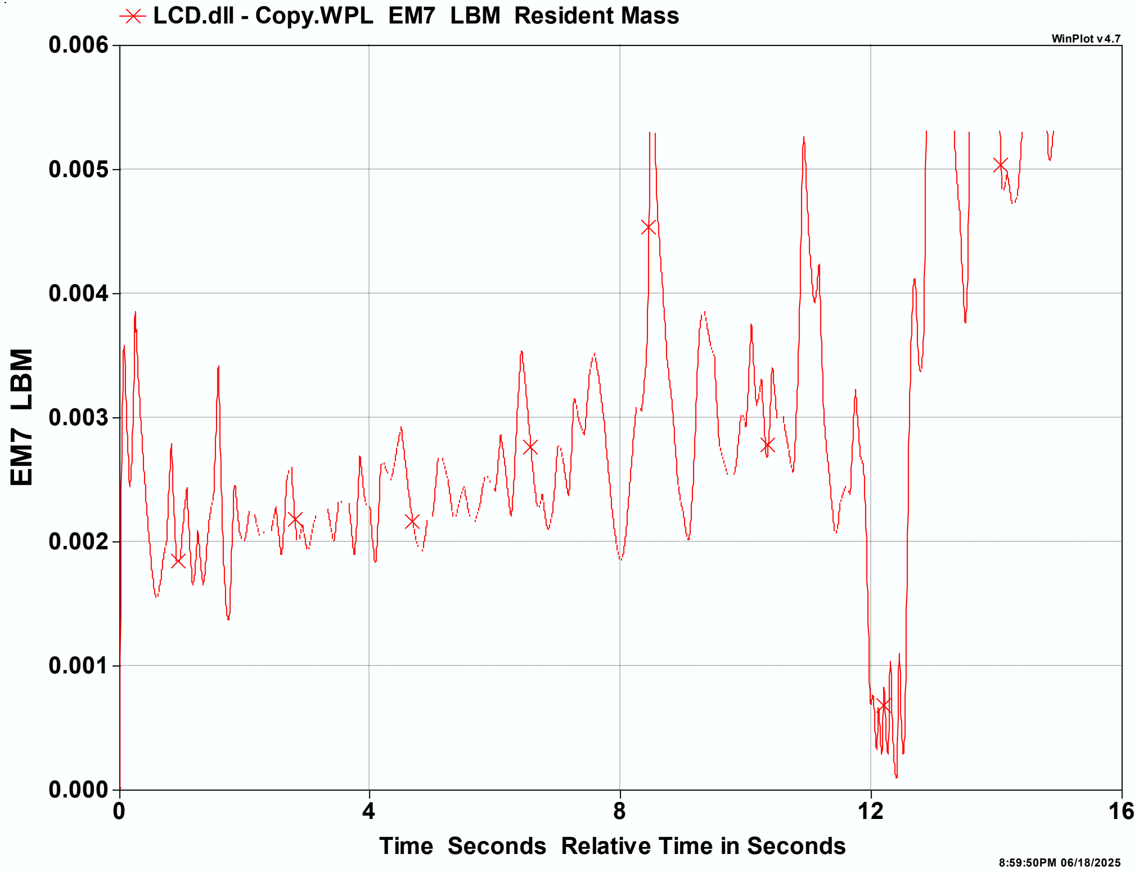

Pulse Flow Upstream

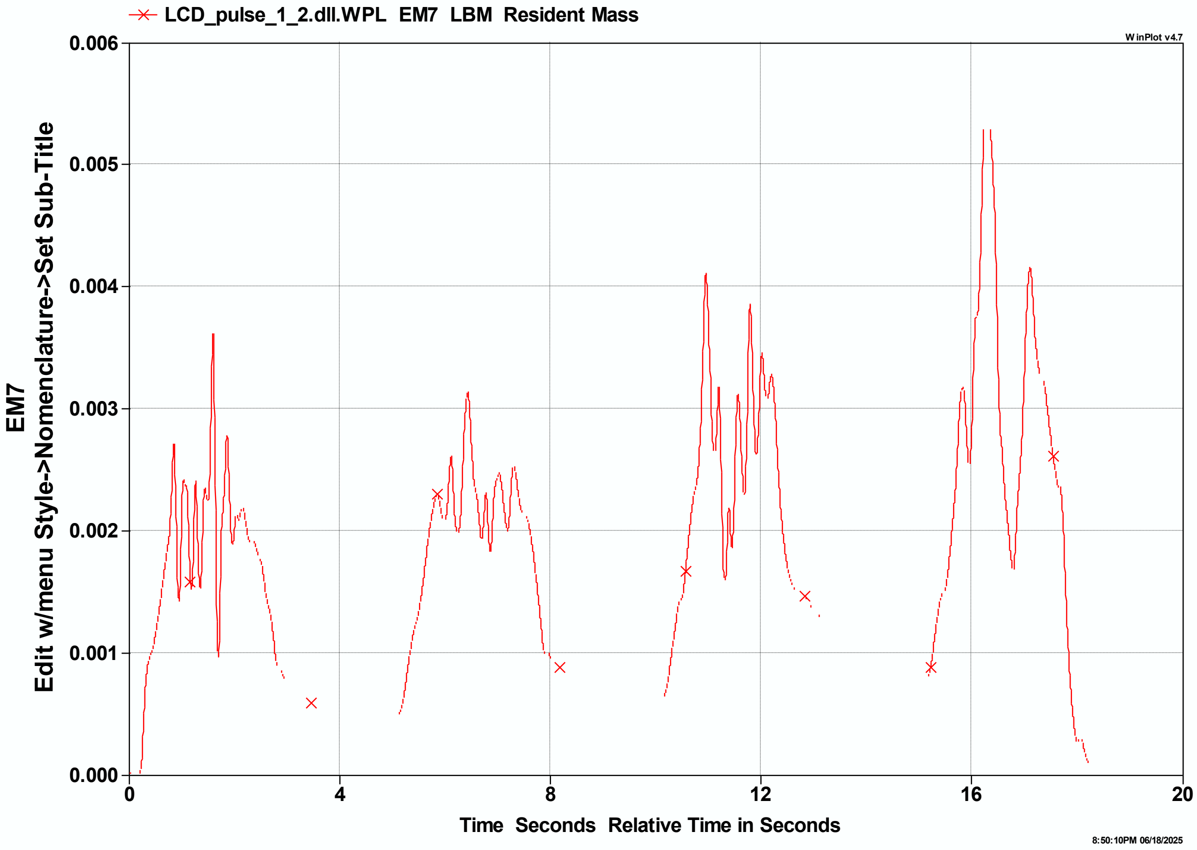

Microfilm Upstream

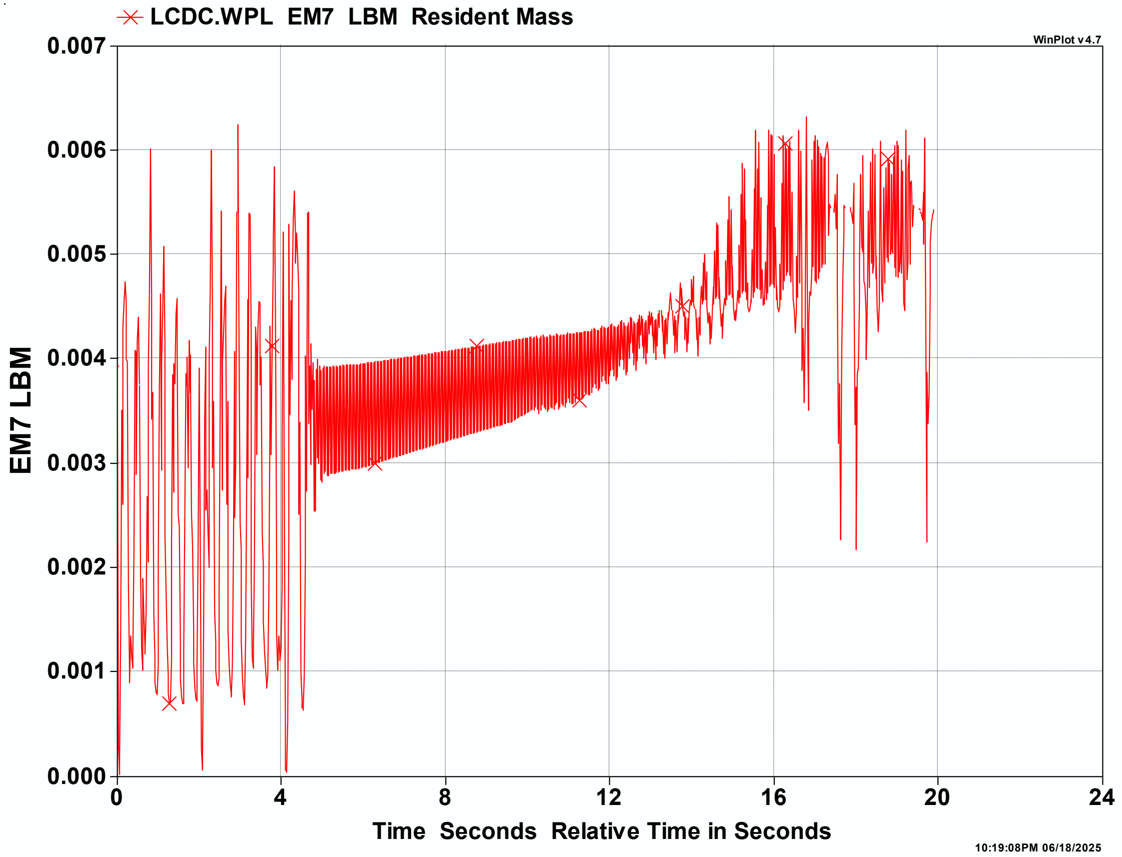

Continuous Flow Upstream

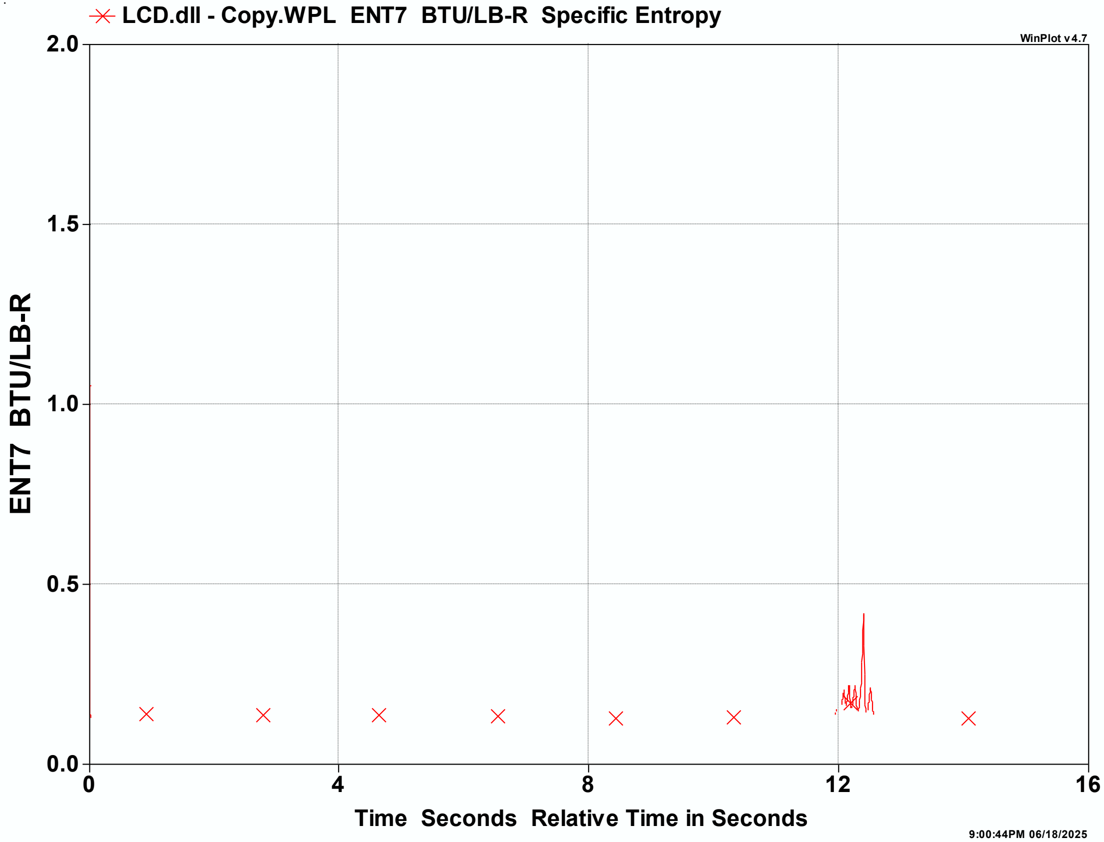

Pulse Flow Upstream

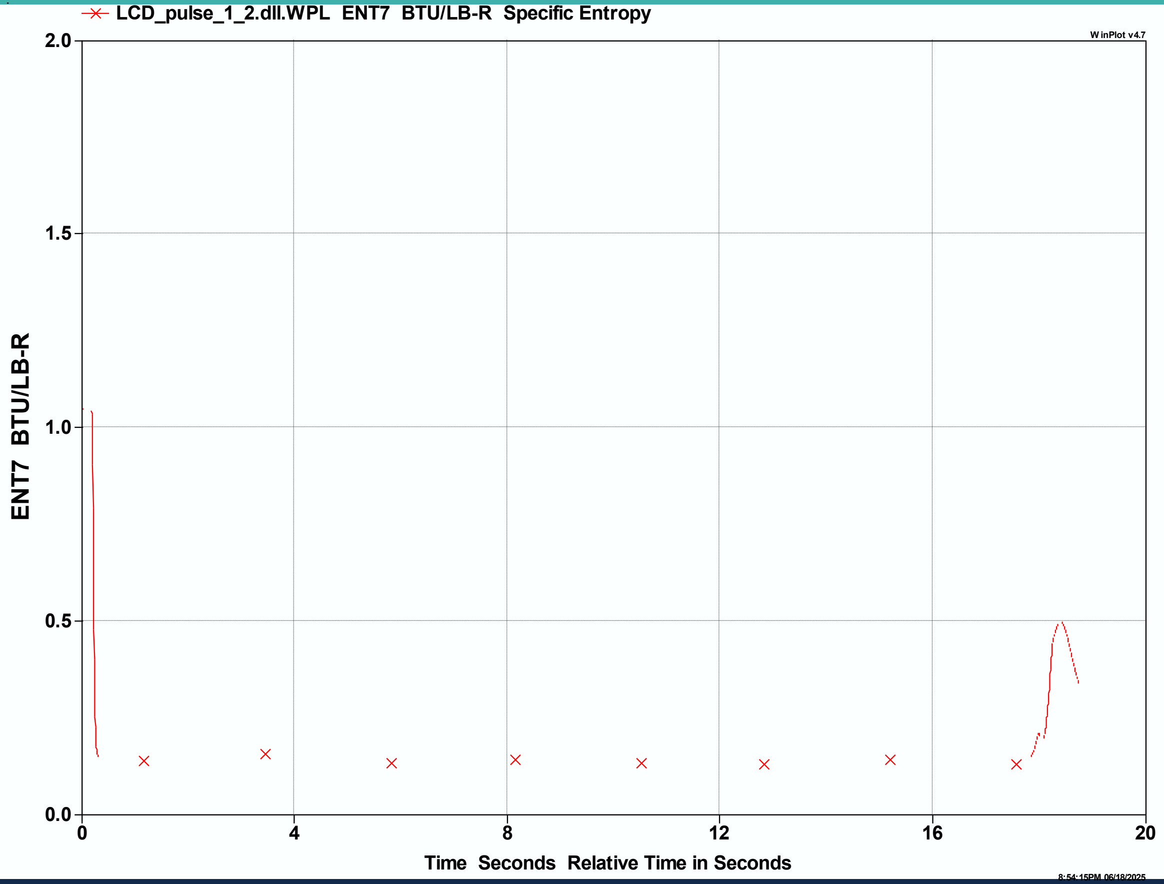

Continuous Flow Upstream

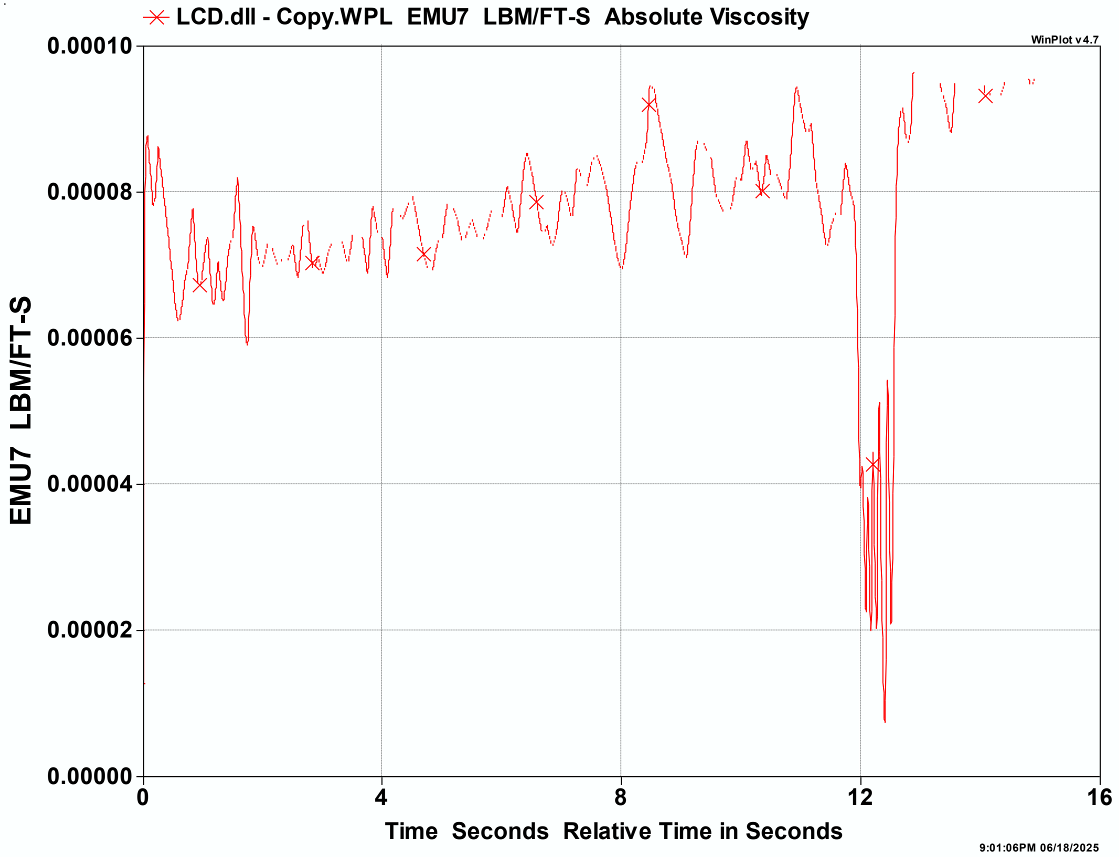

ECLIPSE

Pulse Flow Upstream

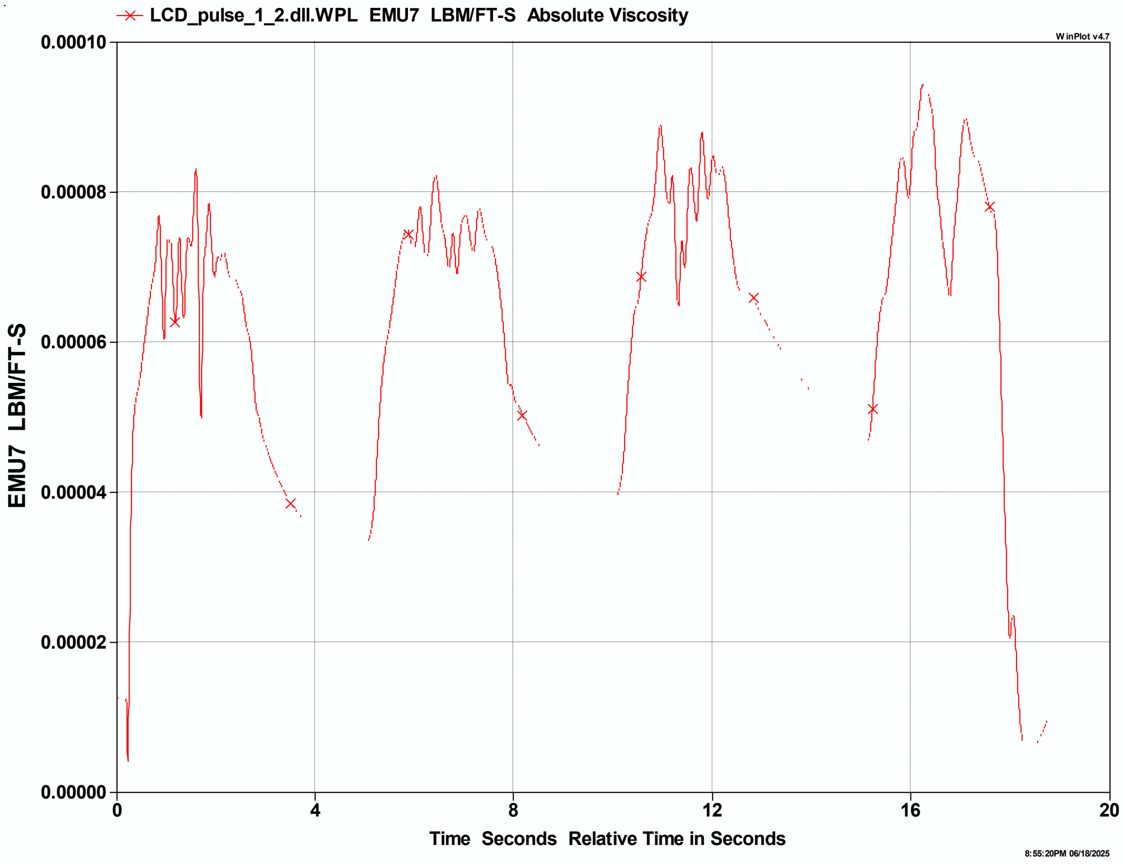

Continuous Flow Upstream

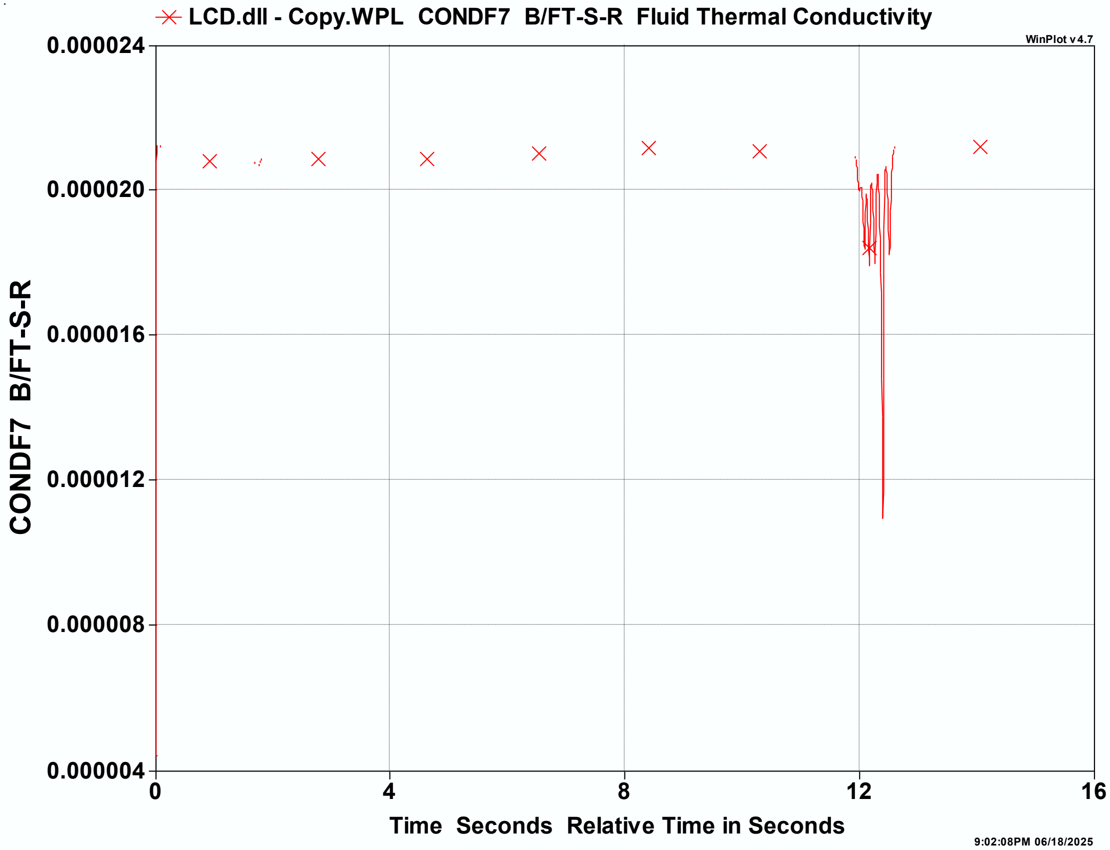

Pulse Flow Upstream

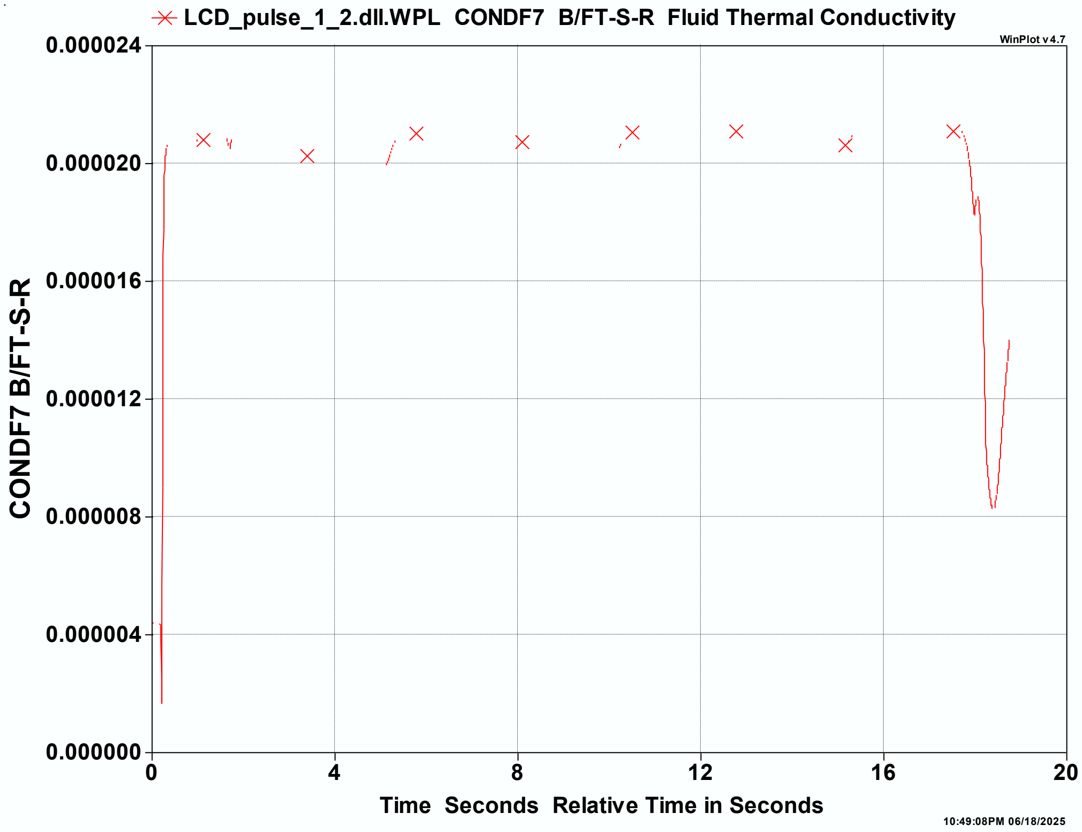

Continuous Flow Upstream

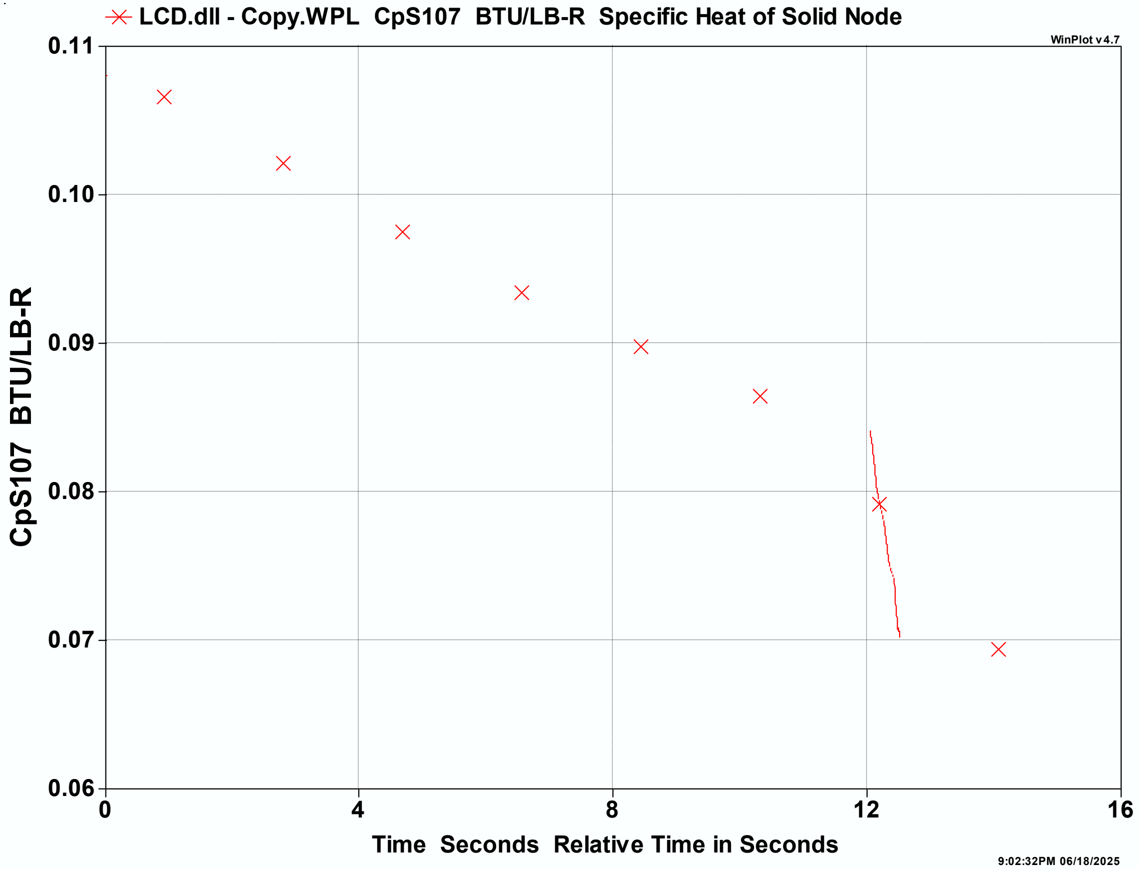

Pulse Flow Upstream

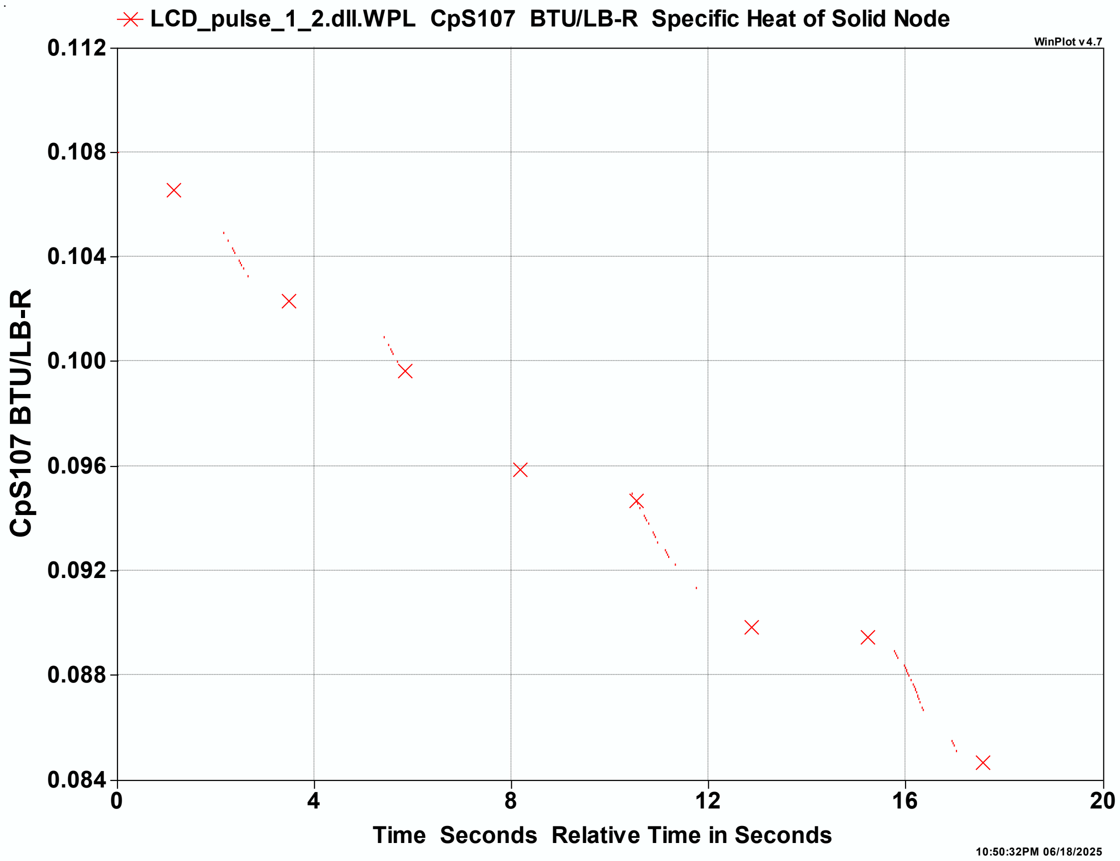

ECLIPSE | Microfilm Upstream

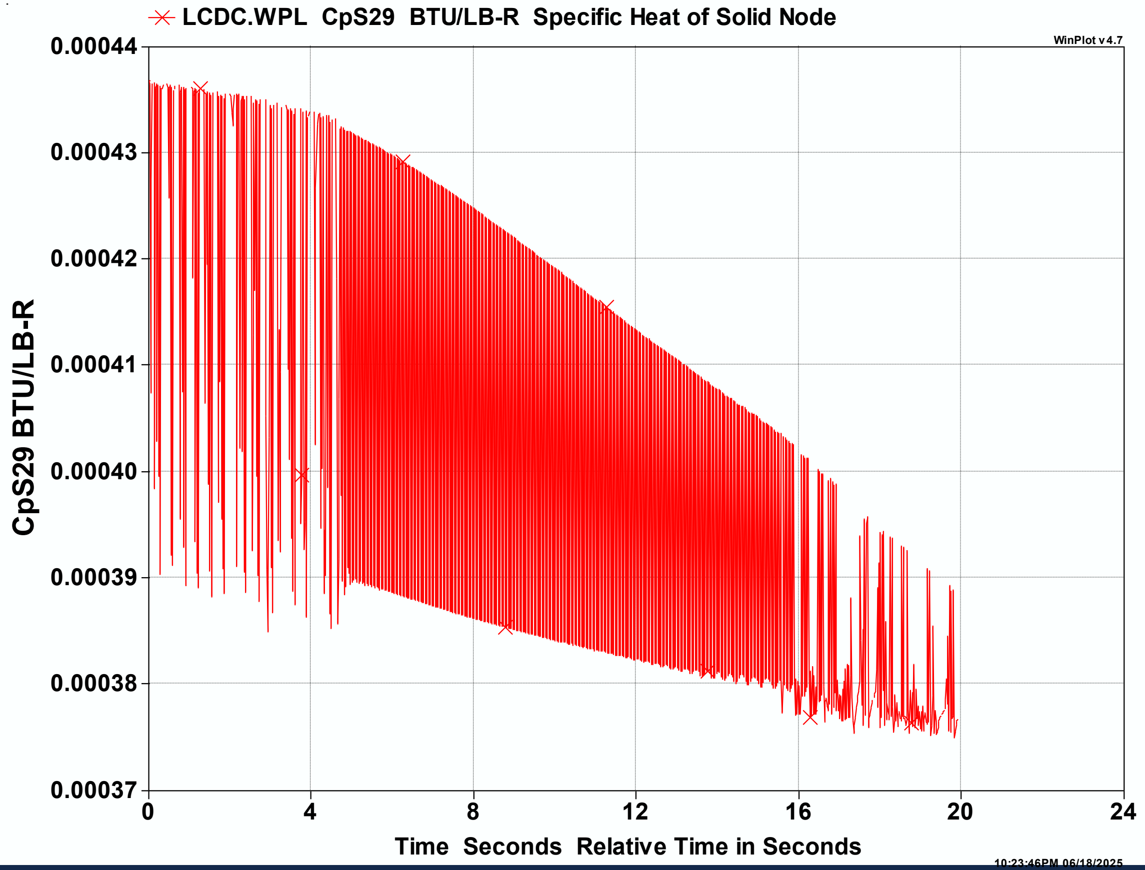

ECLIPSE | Microfilm Upstream

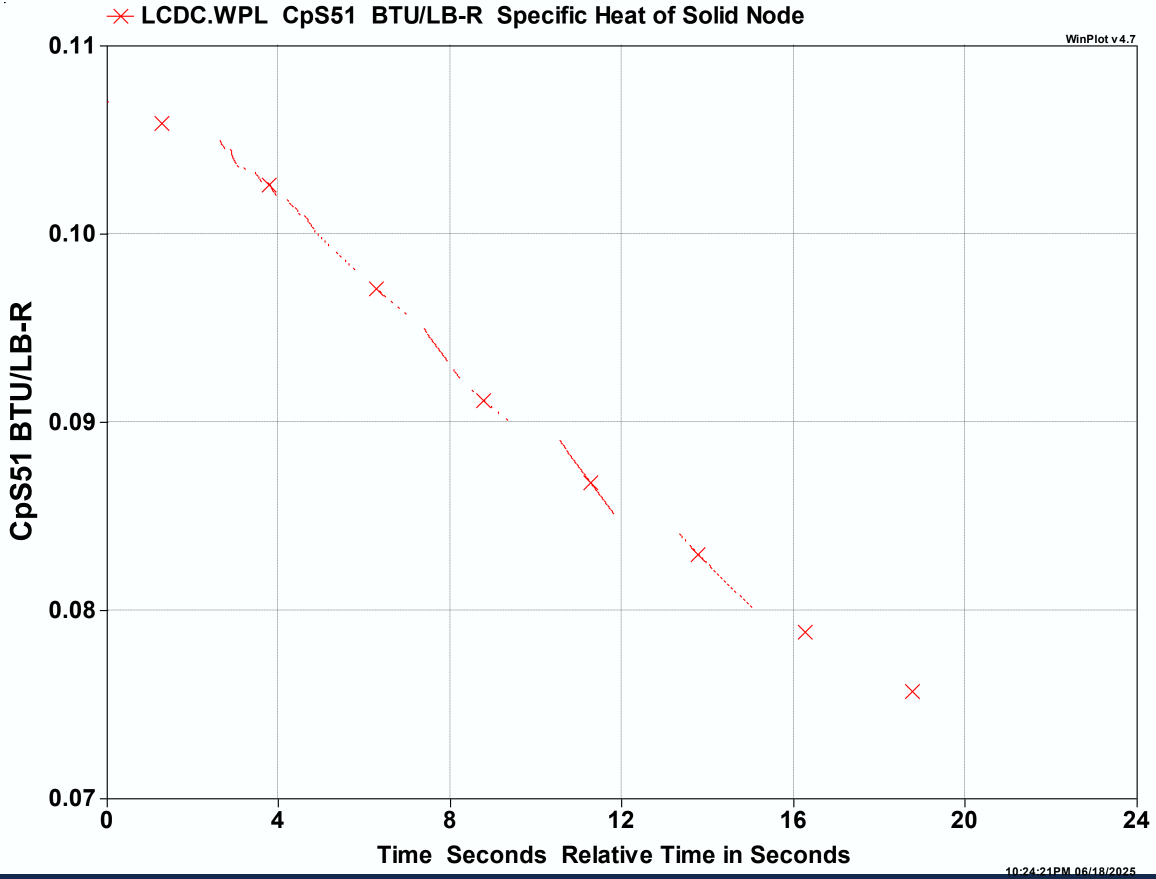

ECLIPSE

Pulse Flow Upstream

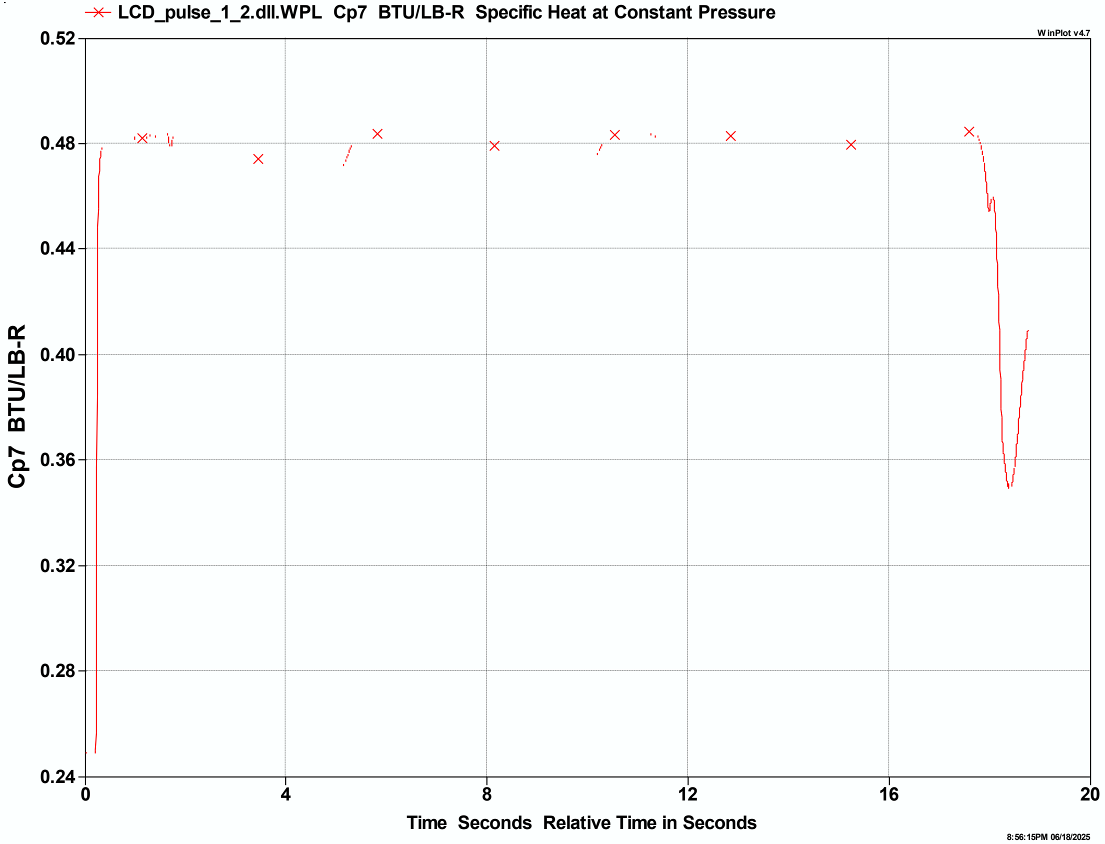

Continuous Flow Upstream

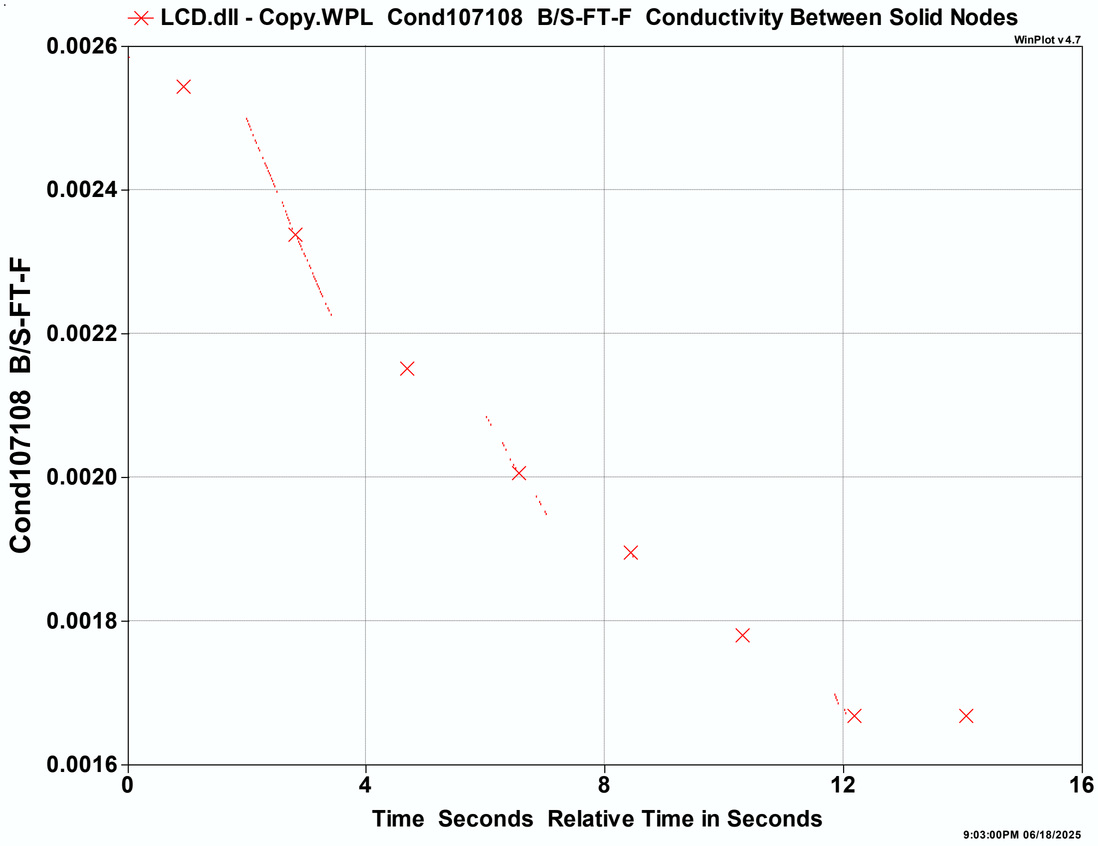

Pulse Flow Upstream

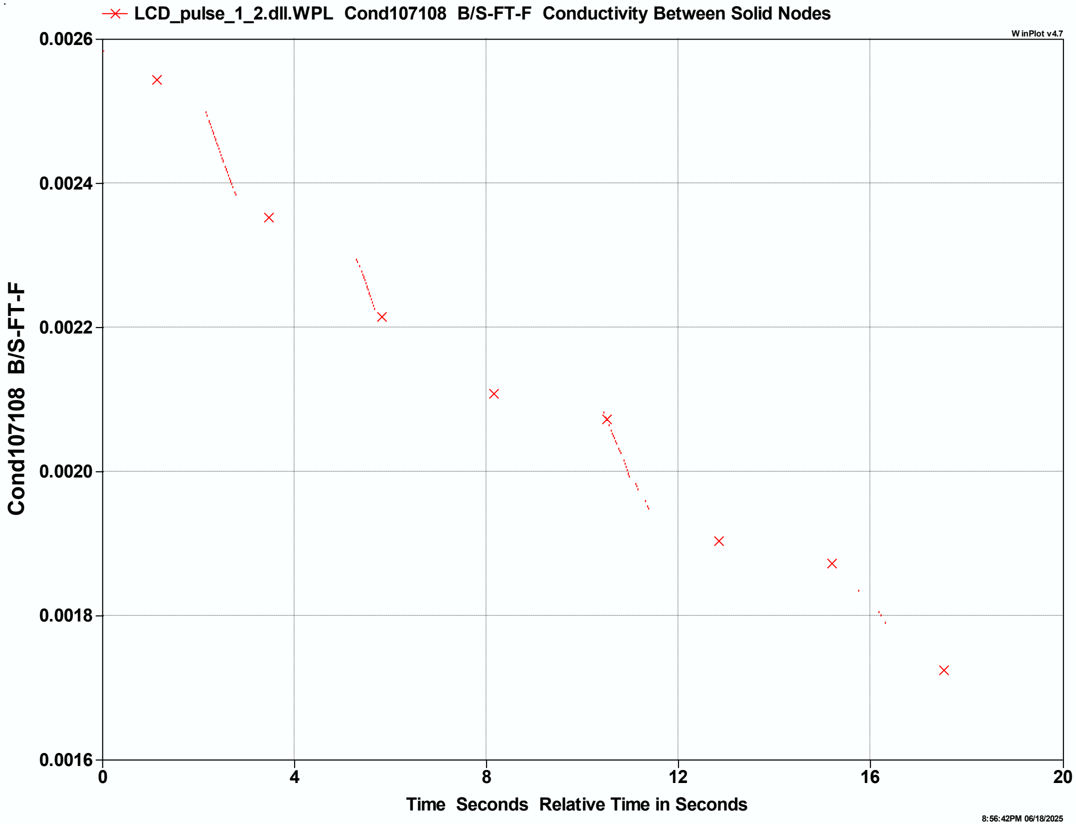

Microfilm Upstream

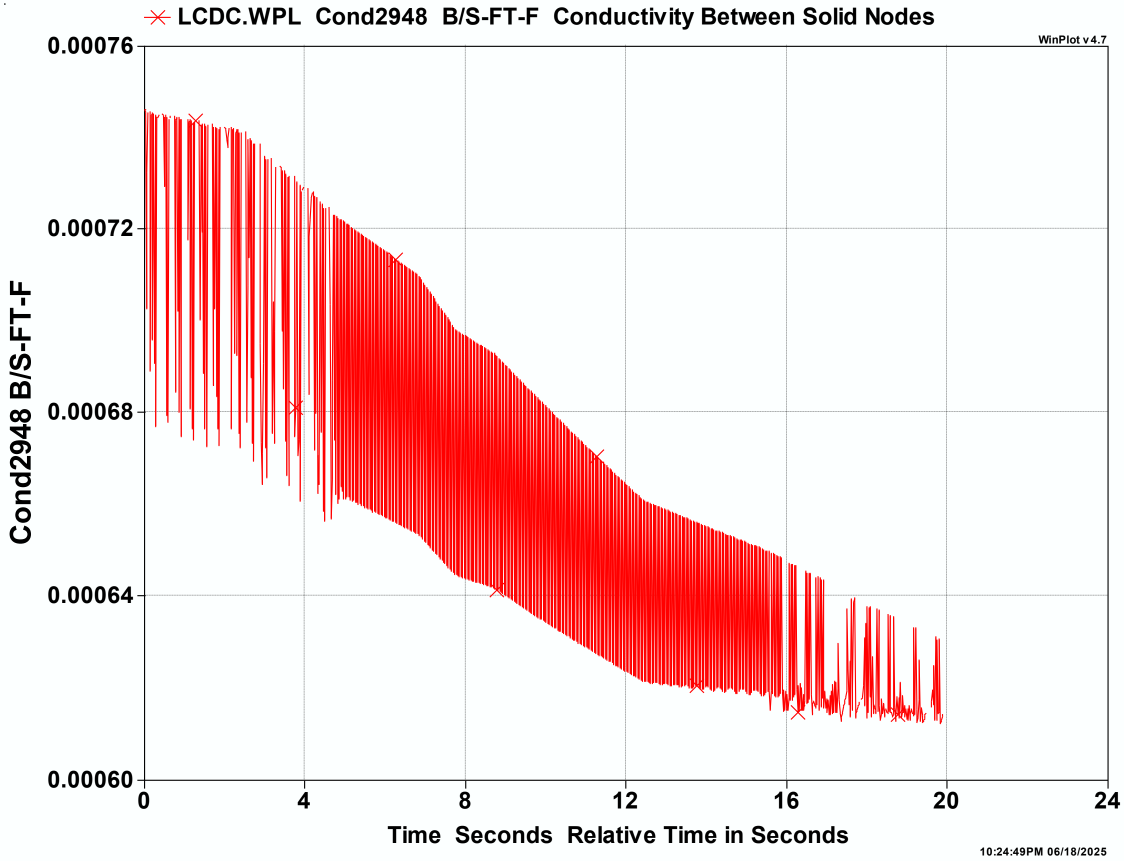

Continuous Flow Upstream

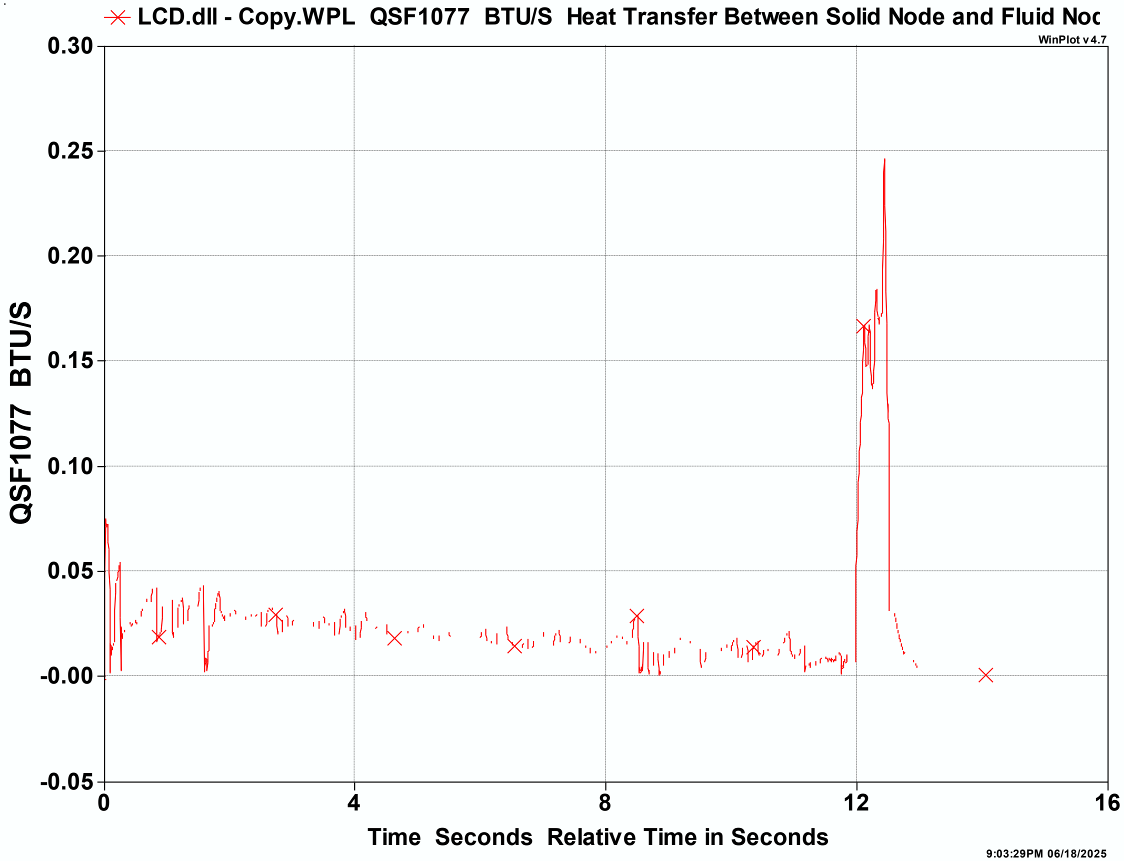

Pulse Flow Upstream

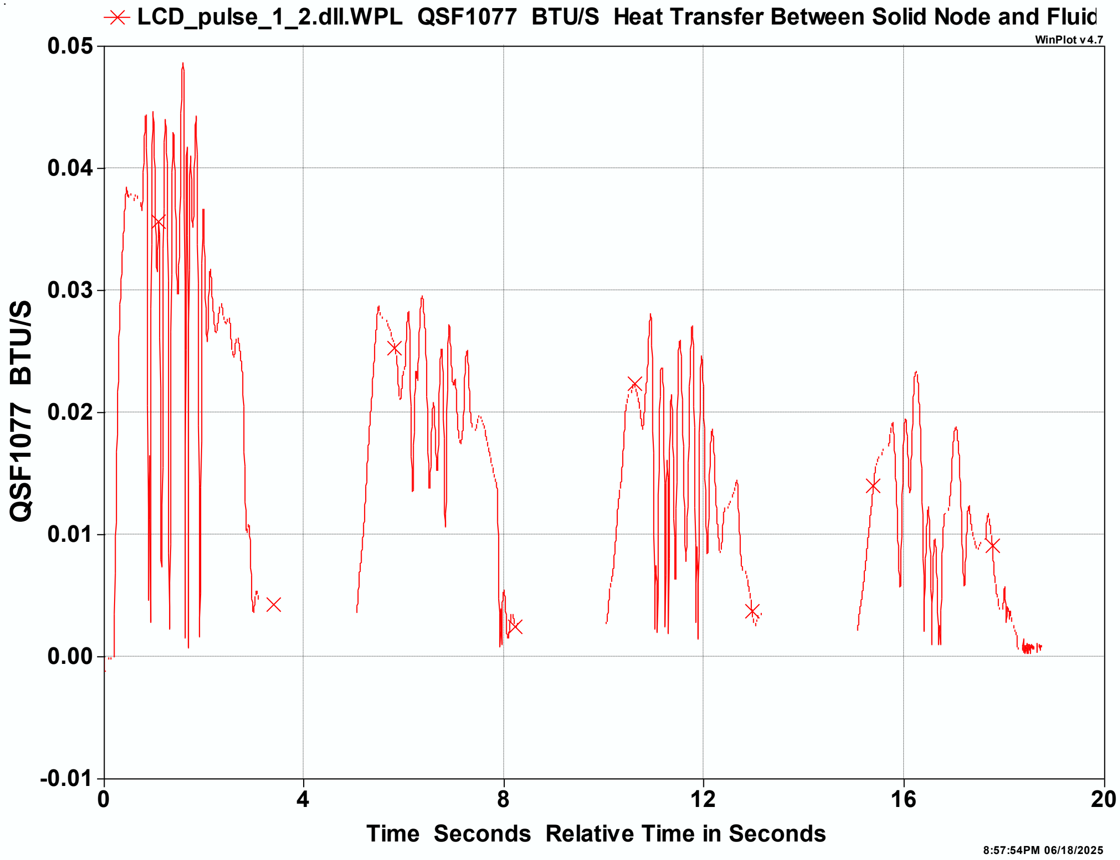

Pulse Flow Upstream

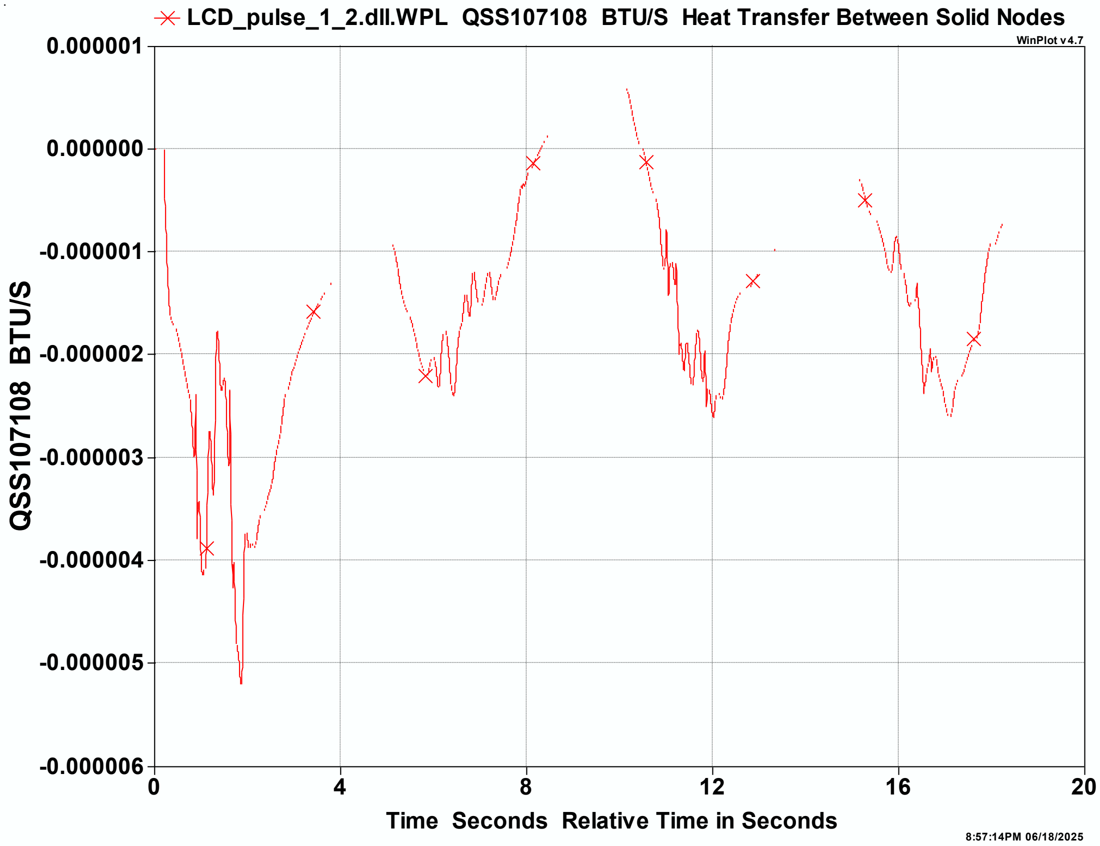

Microfilm Upstream

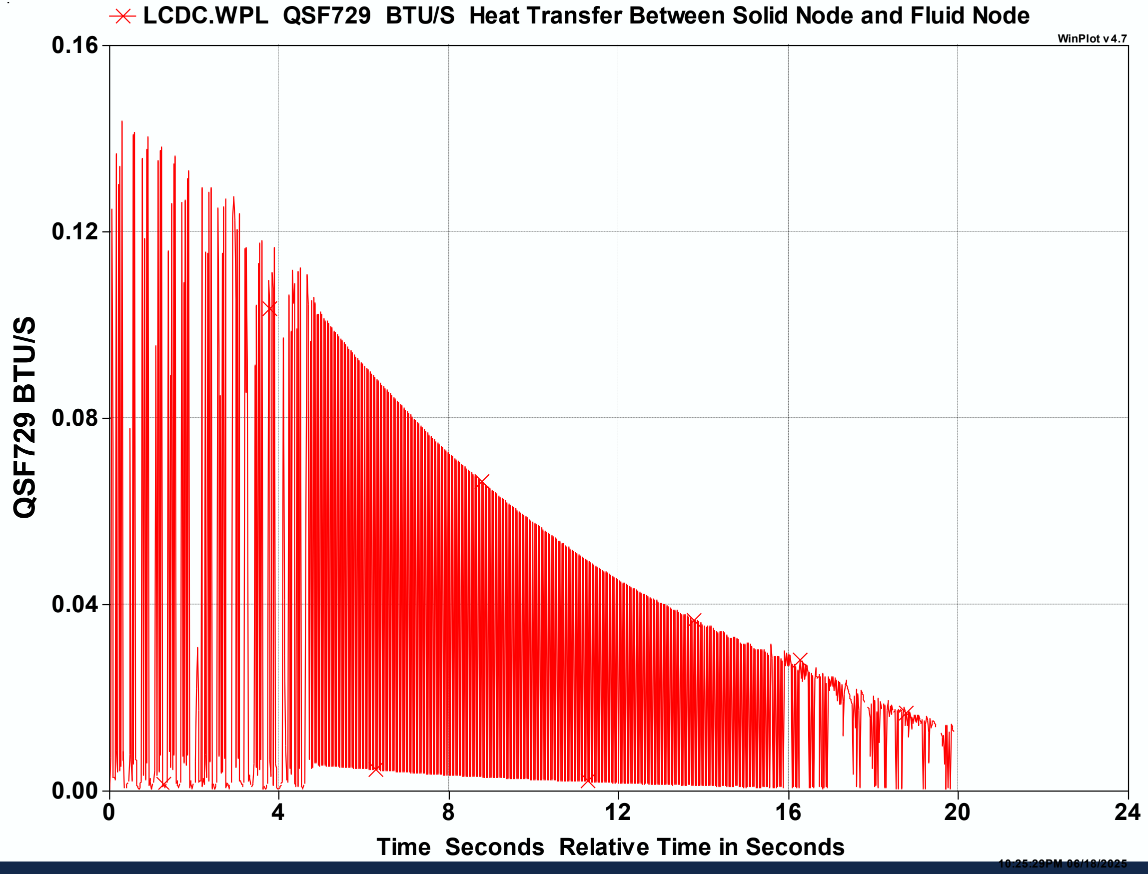

Microfilm Upstream

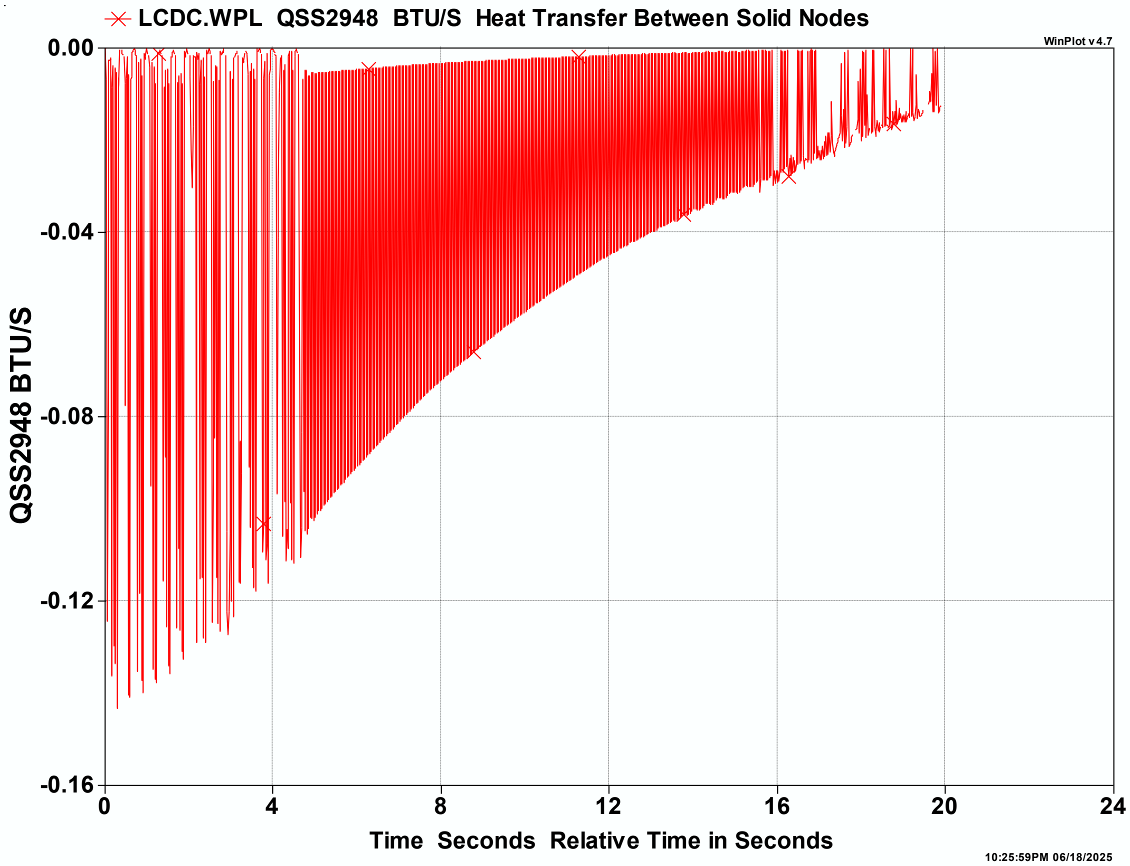

Continuous Flow Upstream

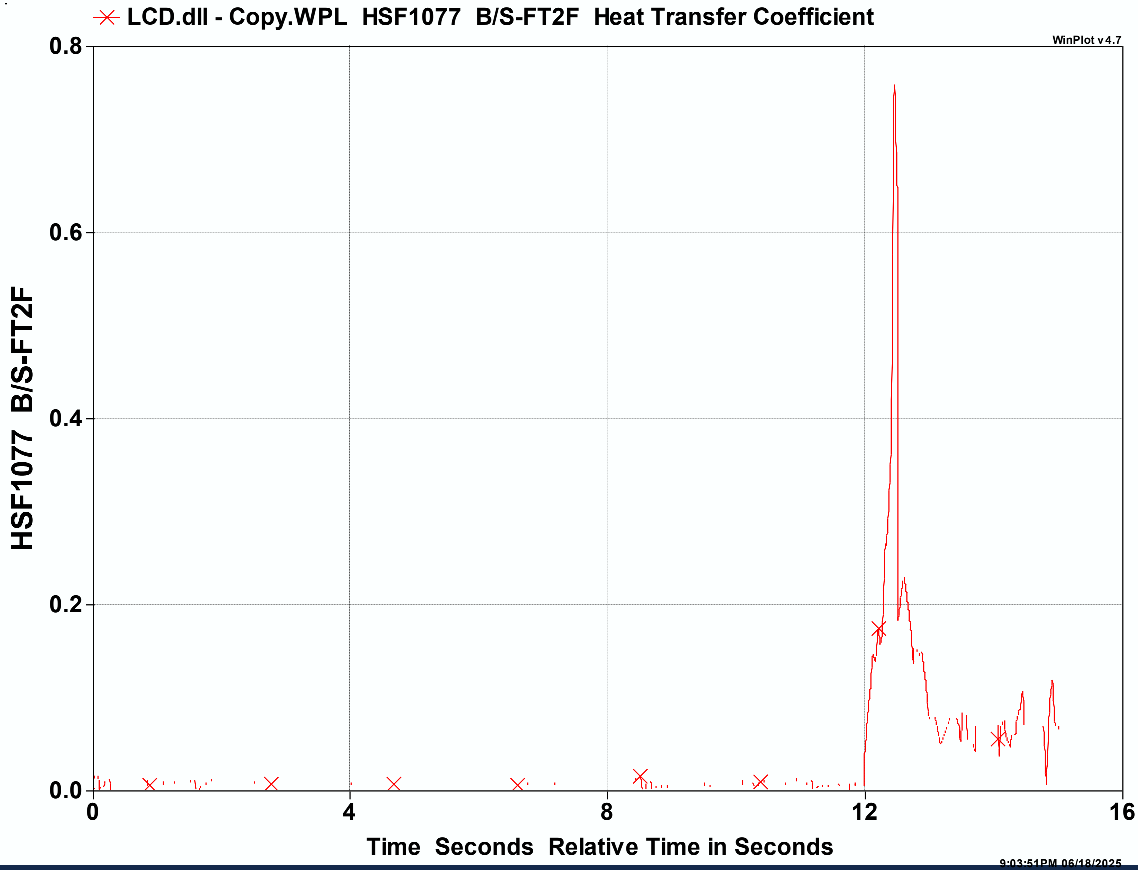

ECLIPSE | Microfilm Upstream

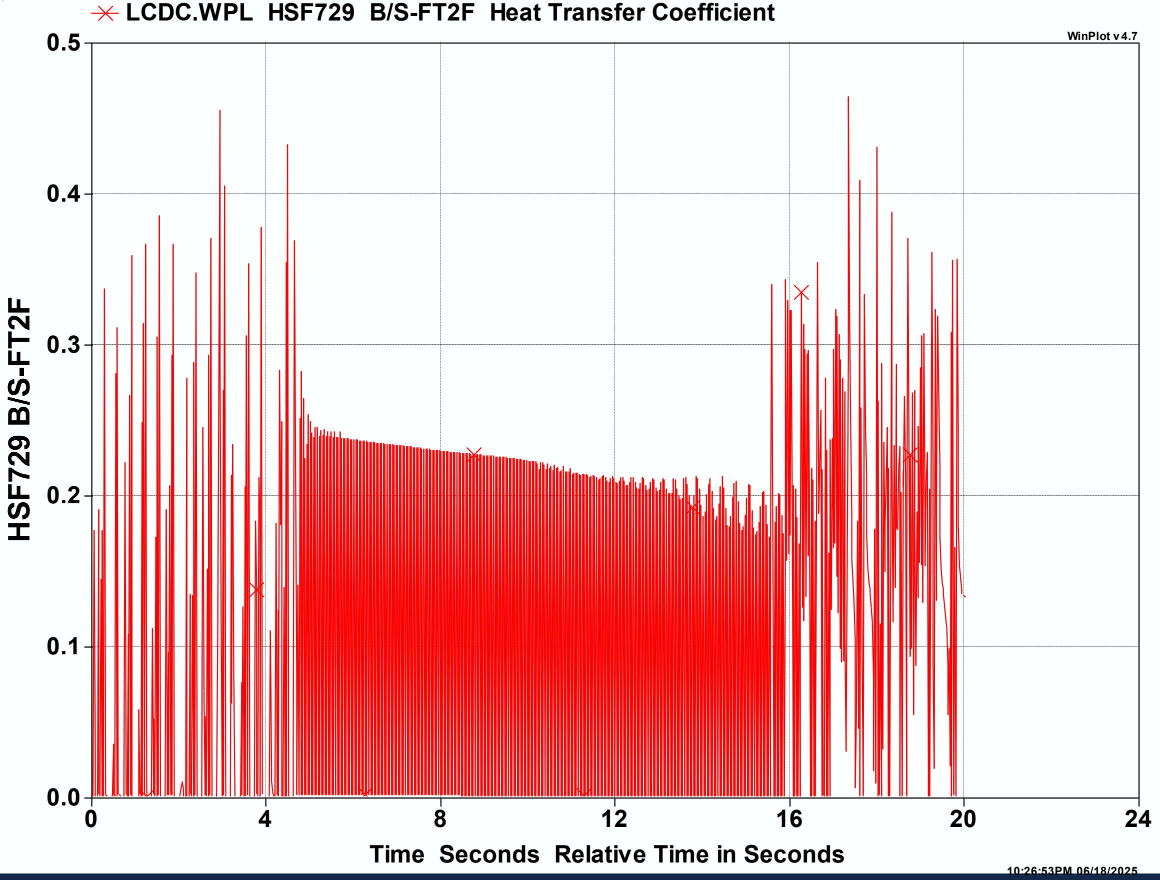

Continuous Flow Upstream

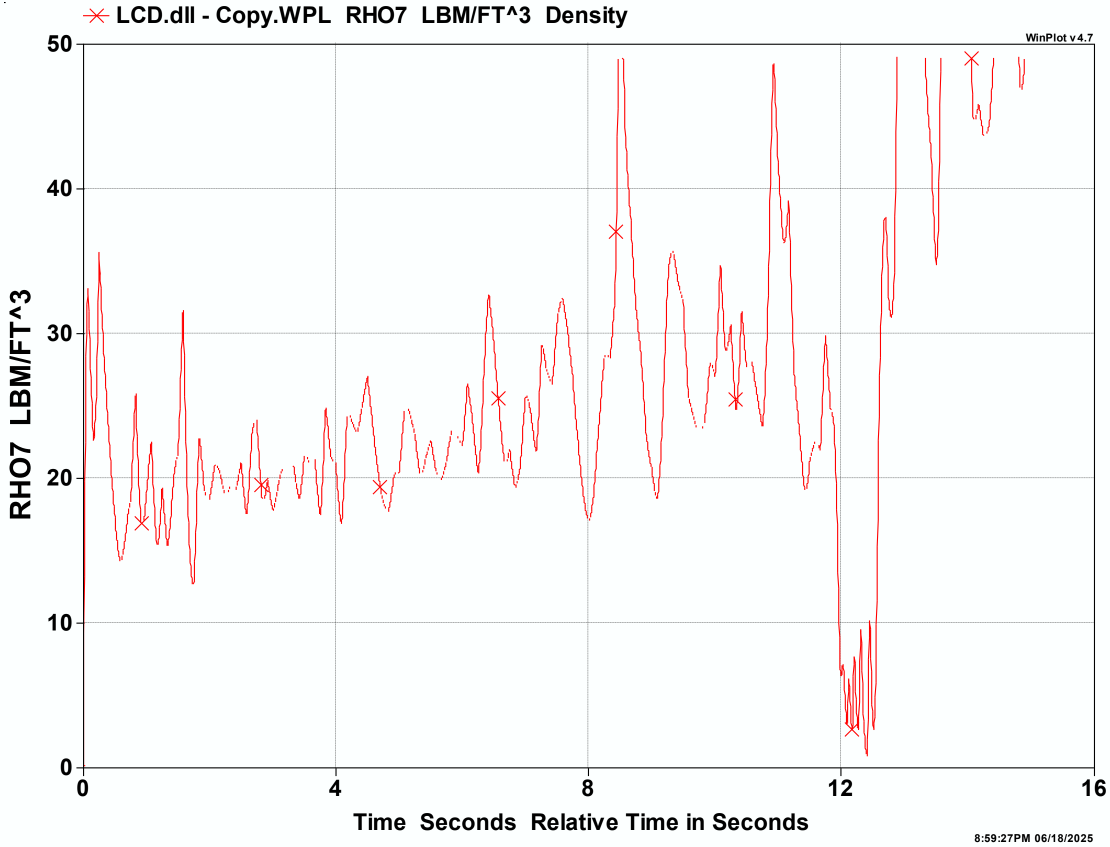

Pulse Flow Upstream

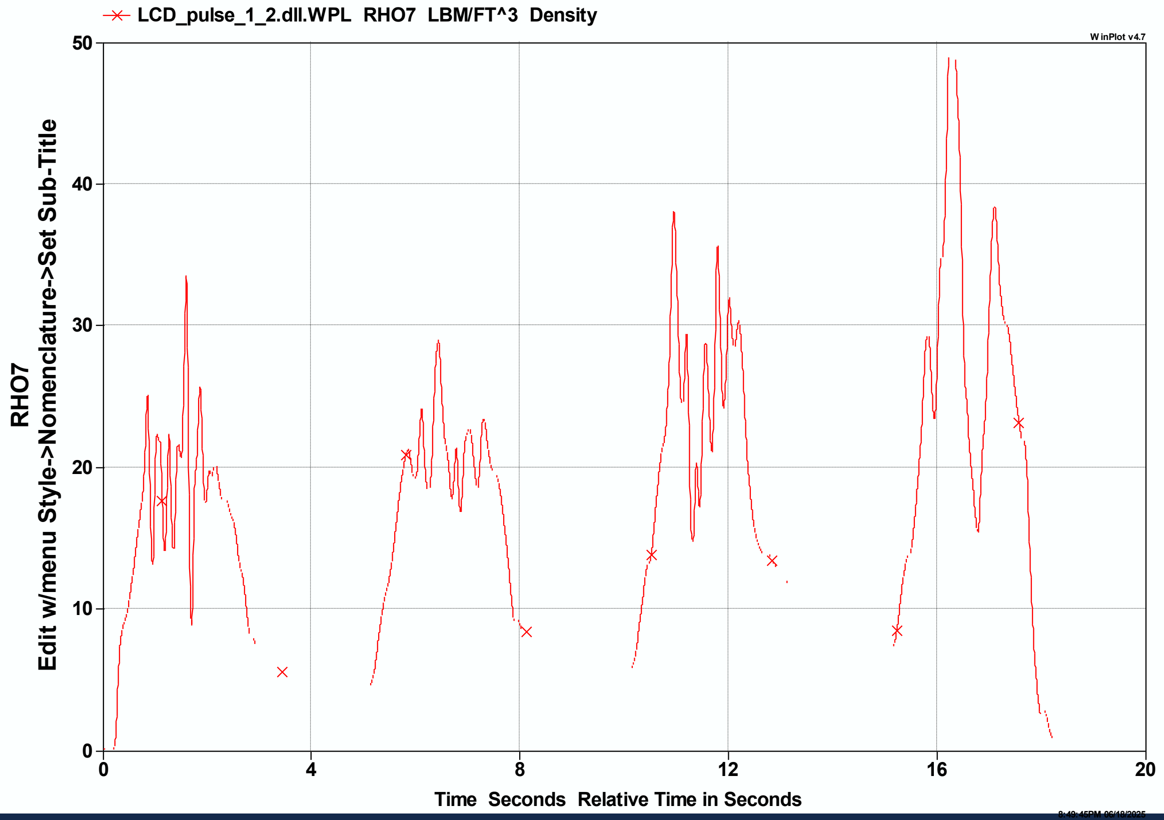

Microflm Upstream

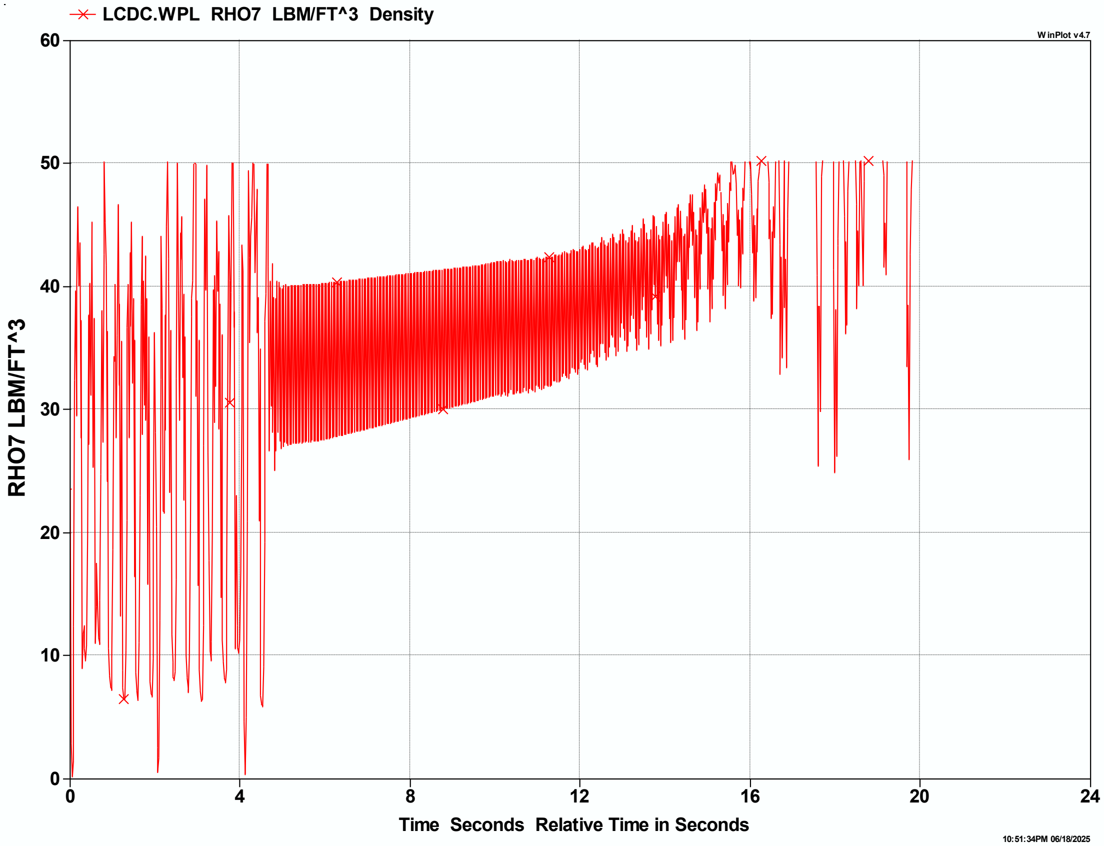

Continuous Flow Upstream

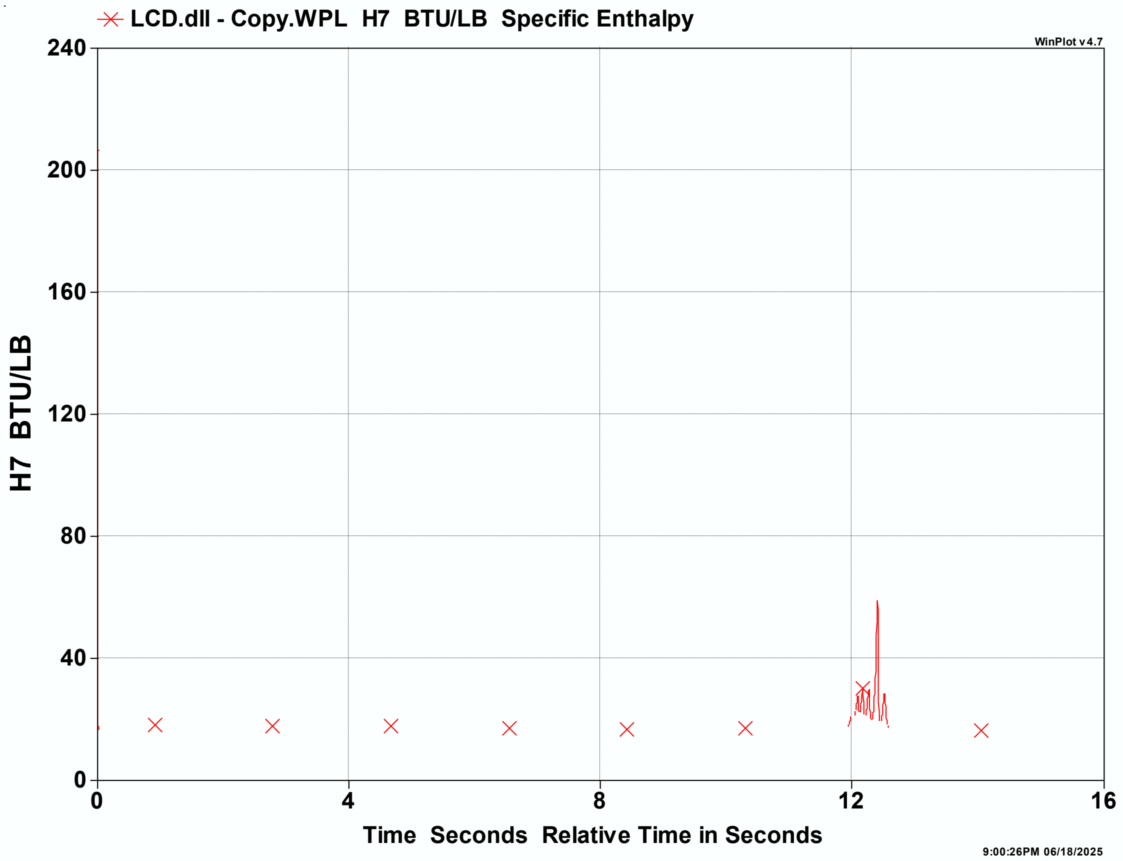

Pulse Flow Upstream

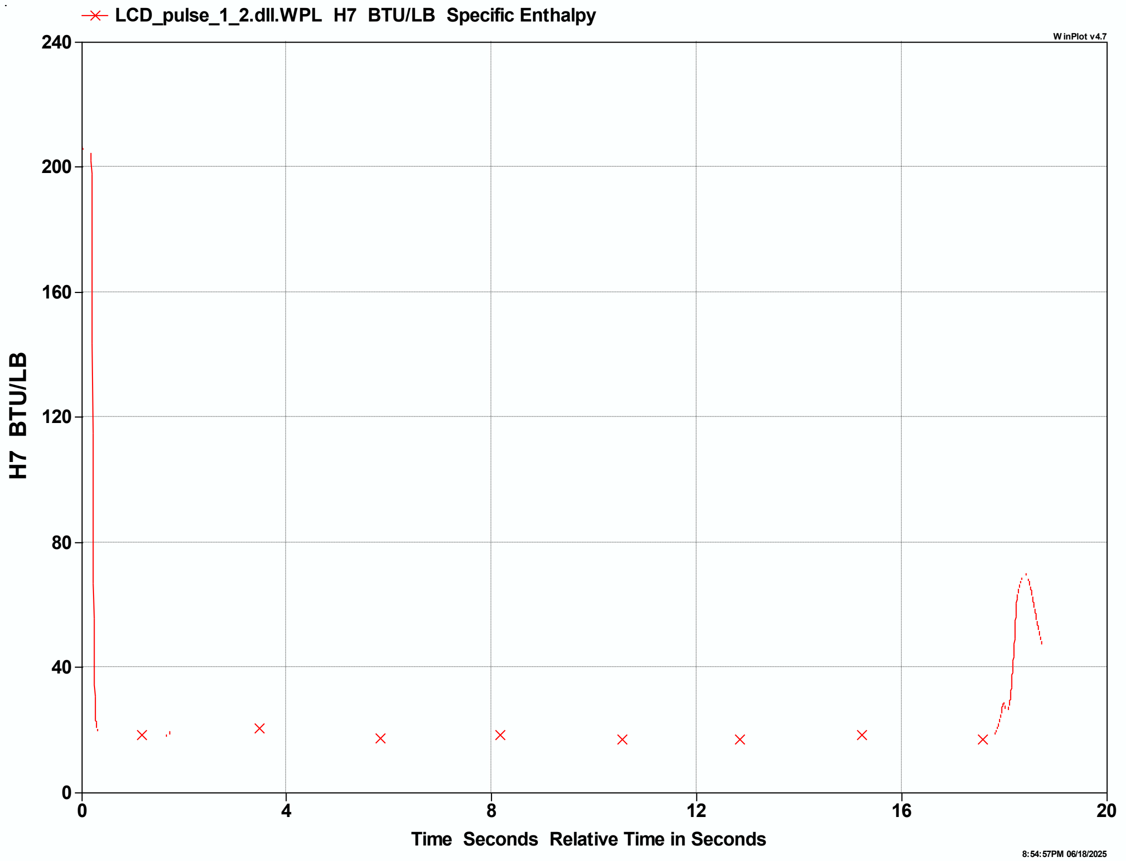

Pulse Flow Upstream

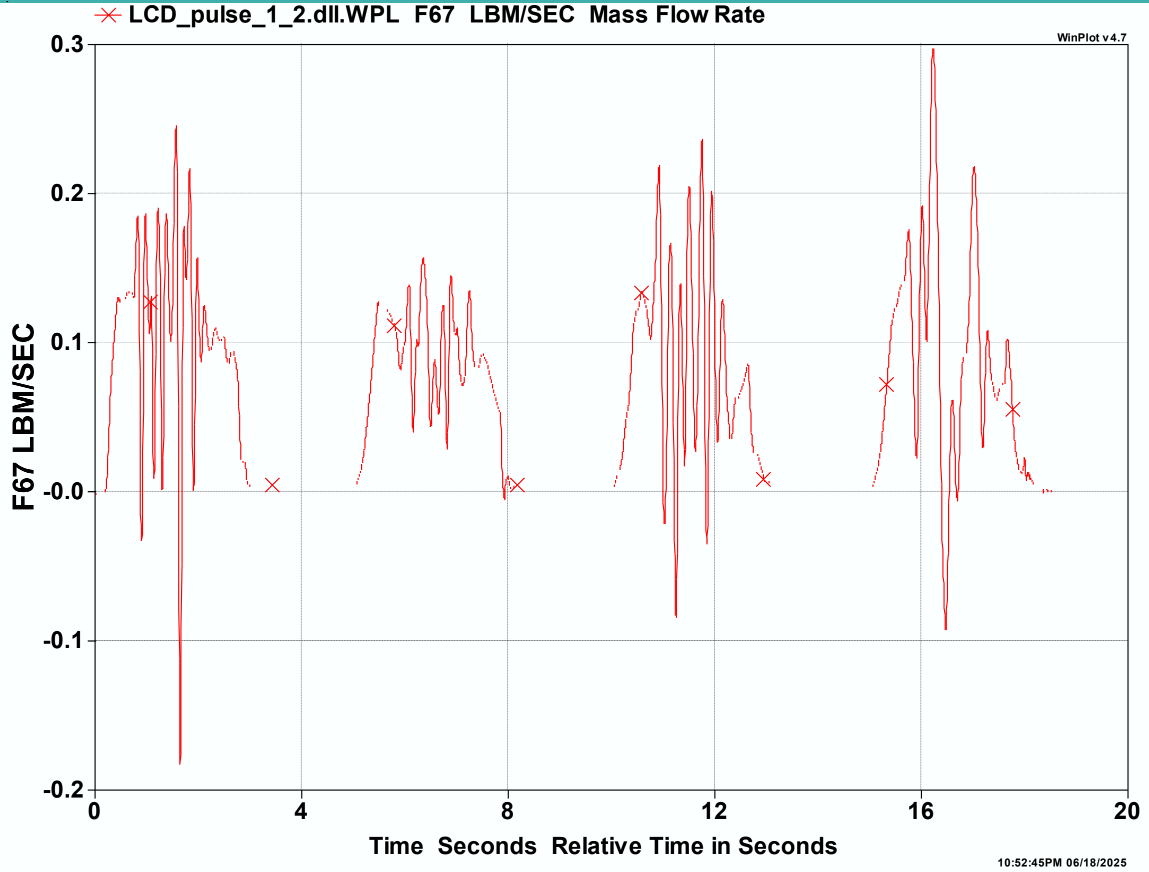

Continuous Flow Upstream

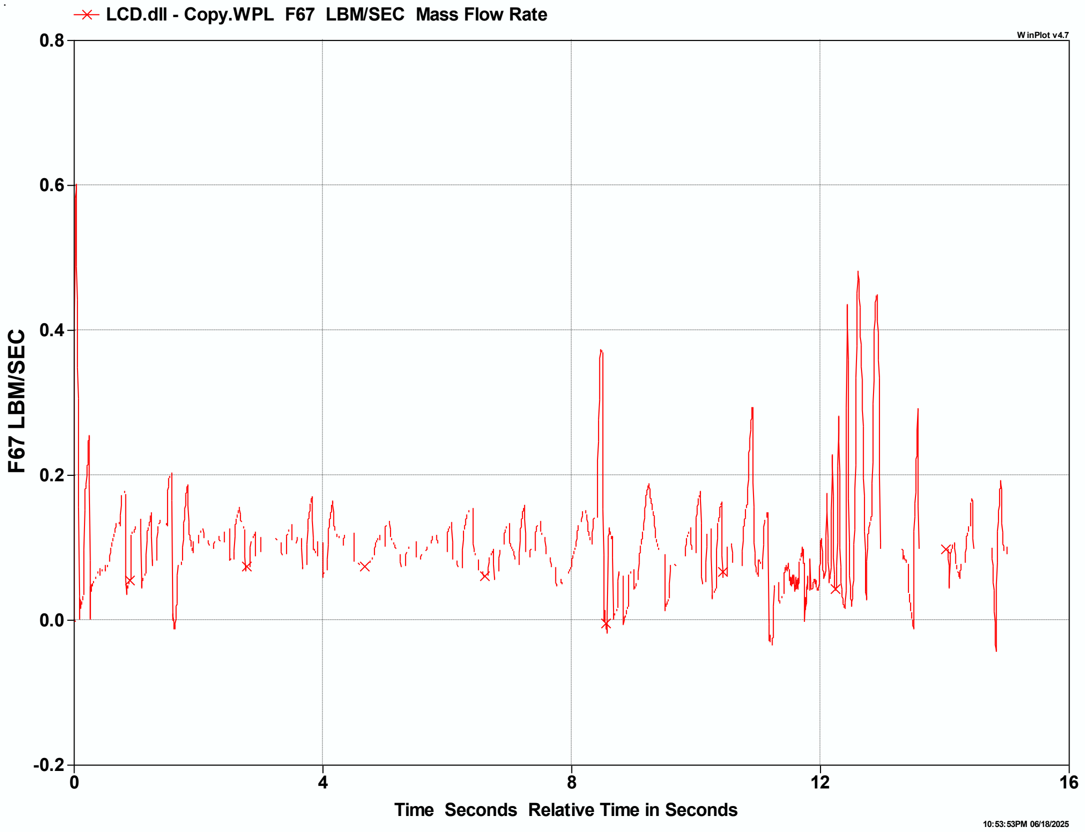

Microfilm Upstream